Università degli Studi di Padova

Dipartimento di Medicina – DIMED

CORSO DI DOTTORATO DI RICERCA IN SCIENZE CLINICHE E SPERIMENTALI
CURRICULUM IN SCIENZE EMATOLOGICHE E GERIATRICHE
XXXV CICLO

Experimental thesis

MYCOSIS FUNGOIDES: NOVEL THERAPEUTIC APPROACHES TARGETING THE CUTANEOUS LYMPHOCYTE ANTIGEN (CLA)

Coordinatore: Ch.mo Prof. Alberto Ferlin

Supervisore: Ch.mo Prof. Mauro Alaibac

Co-supervisore: Dott.ssa Micol Silic-Benussi

Dottorando: Dott.ssa Irene Russo

Table of Contents

.

List of papers discussed in the thesis

Paper I

Targeting the cutaneous lymphocyte antigen (CLA) in inflammatory and neoplastic skin conditions.

Sernicola A, Russo I, Silic-Benussi M, Ciminale V, Alaibac M.

Paper II

Near infrared photoimmunotherapy targeting the cutaneous lymphocyte antigen for mycosis fungoides.

Silic-Benussi M, Saponeri A, Michelotto A, Russo I, Colombo A, Pelizzo MG, Ciminale V, Alaibac M.

Paper III

Near-infrared photoimmunotherapy for the treatment of skin disorders.

Russo I, Fagotto L, Colombo A, Sartor E, Luisetto R, Alaibac M.

Paper IV

The Zebrafish model in dermatology: an update for clinicians.

Russo I, Sartor E, Fagotto L, Colombo A, Tiso N, Alaibac M.

Summary

Background

Mycosis fungoides (MF) is the most common form of cutaneous T cell lymphoma. There are currently few effective therapies for the treatment of MF. Treatments for the early stages generally consist of a skin-directed therapy, and treatments for the late stages are generally systemic, and often combined. Although the initial stages of mycosis fungoides have a moderate clinical course, 30% of patients relapse or prove to be refractory to currently used treatments and are destined to progress to advanced stages of the disease for which, in fact, there is not a curative treatment. Therefore, the development of new therapeutic strategies is fundamental. While the Cutaneous Lymphocyte Antigen (CLA) is strongly expressed by MF tumor cells, it could be a specific molecular target for the treatment of MF.

The aim of the whole PhD project was to investigate novel therapeutic approaches targeting CLA for the treatment of MF. The first specific aim was to investigate the antitumor effect of a CLA-targeted Near-infrared photoimmunotherapy (NIR-PIT) on MF cells and the second specific aim was to investigate the antitumor effect of an antibody-drug conjugate (ADC) consisting of an anti-CLA monoclonal antibody and monomethyl auristatin E (MMAE).

Methods

In vitro validation of anti-CLA monoclonal antibody-based approaches were performed using a MF cell line called Myla CD4+ cell line.

In vivo studies are ongoing on zebrafish embryo model of MF created by the injection of Myla CD4+ cells into the yolk sac at 2 days post fertilization.

Results

Treatment with anti-CLA monoclonal antibody alone or near infrared light irradiation alone exhibited very modest pro-death effects, while the combination of the two induced a substantial increase in death in the MF cell line showing that CLA-targeted NIR PIT has a marked anti-tumor effect *in vitro*. Conversely, the anti-CLA-MMAE antibody drug conjugate exhibited *in vitro* lower cytotoxic activity compared to anti-CLA monoclonal antibody or MMAE alone.

In vivo validation phases studies are ongoing to investigate the efficacy of these anti-CLA monoclonal antibody-based approaches. Preliminary data are encouraging but are still under evaluation.

Discussion

An anti-CLA monoclonal antibody-based approach may represent a novel and highly selective treatment for this disease.

While CLA-targeted NIR-PIT shows a marked anti-tumor effect on MF cells *in vitro*, it is an attractive candidate for in vivo studies and ultimately for clinical trials.

The anti-CLA-MMAE ADC shows low cytotoxicity activity *in vitro* which could be explained by the lack of internalization of the ADC into the cells. However, it has recently been demonstrated that *in vivo* non-internalizing antibodies may have potent anti-cancer activity thanks to proteolytic release of MMAE in the subendothelial extracellular matrix. Thus, anti-CLA-MMAE ADC may be effective *in vivo*.

The xenotransplantation experiments performed to evaluate the proliferation of MF cells in zebrafish embryos have given very positive and extremely encouraging results, confirming the possible use of this animal species as a model for the study of this pathology.

Introduction

Mycosis fungoides

Epidemiology and clinical presentation

Cutaneous T-cell lymphomas (CTCLs) are a group of extranodal non-Hodgkin lymphomas with an overall incidence of 10.2 per million persons [1,2].

Mycosis fungoides (MF) is a low-grade cutaneous lymphoma with primary cutaneous involvement accounting for more than half of all primary cutaneous lymphomas with an incidence of 5.6 per million persons [3, 4].

The risk of MF is associated with age, gender and race, with relatively higher prevalence among the elderly, blacks and males [5].

Clinically, MF is characterized by long-standing, scaly, patch lesions preferentially involving the buttocks and body areas infrequently exposed to sunlight and slow evolution over years from patches to plaques (early-stage) and in some patient to tumors or erythroderma (advanced-stage MF patients) [6].

MF is defined histologically by an initial skin infiltration with small to medium sized cells characterized by cerebriform nuclei and epidermotropism [7]. These cells are clonally derived malignant CD4+CD45RO+- phenotype T lymphocytes showing expression of the cutaneous lymphocyte antigen (CLA) [8, 9]. The diagnosis is often made after several aspecific biopsies.

Pathogenesis

MF and Sezary Syndrome (SS) arise from skin tropic memory CD41 T-cell (CD81 and CD4– CD8- subtypes may also be observed); but demonstration of different T-cell surface phenotypes and molecular profiles support the hypothesis that these malignancies originate from distinct memory T-

cell subsets: the skin resident memory T-cell (TRM) in MF and the skin-tropic central memory T-cell (TCM) in SS [10]. The average adult skin contains about 20 billion T-cell [11]. These T-cell are normally present in noninflamed human skin [12]. Most of these T-cell are memory T-cell; less than 5% are naïve [11]. Naïve T-cell reside in the blood or lymph nodes [13]. If naïve T-cell first encounter antigen in skin-draining lymph nodes, they proliferate clonally as effector T-cell and differentiate to express the skin homing addressin cutaneous lymphocyte antigen (CLA) and the C-C chemokine receptor 4 (CCR4) (Figure 1)[13].Once these effector T-cell eliminate their cognate antigen, they differentiate into memory T-cell (Figure 1)[13-15]. Skin TCM cells are CCR41/CCR71/L-selectin1, which allows for circulation in skin, blood, and lymph nodes [15].
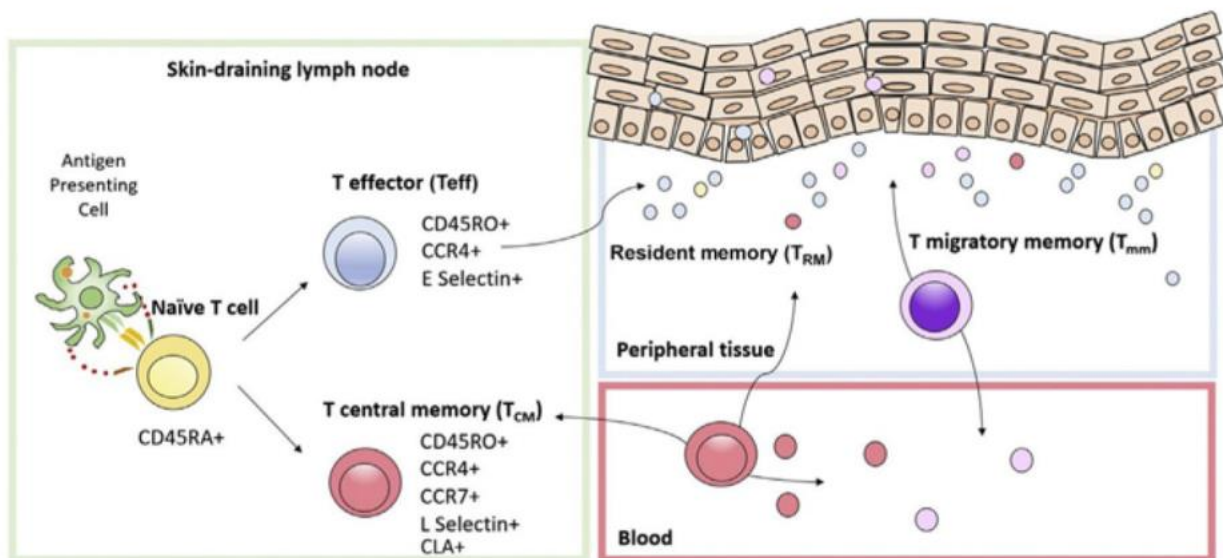

Figure 1. Skin-tropic T-cell subtypes. Naïve T-cell differentiate into effector memory and central memory T-cell after binding to their cognate antigen on antigen presenting cells in skindraining lymph nodes. Expression of surface ligand CCR4 determines their skin homing ability. Expression of CCR7/L-selectin determines their ability to re-circulate between blood and lymph node.

Skin resident TRM cells are CCR41/CLA1 and lack CCR7 and L-selectin. They rarely circulate out of the skin [15]. A subset of T-cell, termed the migratory memory T-cell (TMM), express CCR7 but

not L-selectin and perhaps represent an intermediate phenotype recirculating more slowly out of the skin to blood compared with the TCM [15,16].

Campbell and colleagues17 showed that MF malignant T-cell are CCR41/CLA1/L-selectin-/ CCR7- (TRM), whereas SS malignant T-cell are CCR41/L-selectin1/CCR71 (TCM). The molecular behavior of these T-cell types correlates with the clinical presentation of their malignant counterpart. Skin TRM are nonmigratory populations, and clinically patients with MF have fixed skin lesions with discrete borders [13, 17]. In contrast, TCM recirculate between skin, blood, and lymph node; clinically patients with SS have diffuse erythema and leukemic disease [10, 16]. Patients with a TMM phenotype have ill-defined but discrete skin lesions [15, 16].

Management of MF

Management is based on stage directed treatment with early stage MF (I1-IIA) using skin directed therapies (SDTs), including topical corticosteroids (TCS), phototherapy, topical chemotherapy or retinoids, and radiotherapy (Table 1)[18]. There is no specific algorithm for management of early stage disease and treatments should be tailored according to individual patients needs and their side-effect profile.

Skin-Directed Therapies	Overall Response Rate (%)
Topical superpotent corticosteroids	75–95
Bexarotene gel	50–75
Nitrogen mustard/mechlorethamine HCl gel	50–90
Imiquimod cream	50
Tazarotene cream	58
Narrow-band UVB	54–90
PUVA	85–100
Radiation therapy (local external electron beam, brachytherapy, total skin electron beam therapy)	—

Abbreviations: HCl, hydrochloride; PUVA, psoralen UVA.

Table 1: Skin-Directed Therapies for mycosis fungoides.

dvanced stage (IIB–IV) or refractory MF often requires systemic treatments in combination with SDT for symptomatic relief. The impact of SDT in preventing MF progression is not fully known [19], and is primarily used as a palliative approach, aiming to improve the patient's quality of life [19]. SDTs may improve, pruritus, pain or clinical appearance. There is no evidence that more aggressive therapies prolong survival (Table 2).

The only potential curative therapy is allogenic hematopoietic stem-cell transplantation.

Systemic Therapies	Overall Response Rate
Bexarotene	ORR 45%, CR 13%[14]
IFN a	ORR 64%; CR 27% in stage IA–IVA[15]
Romidepsin	ORR 38%, CR 6%[16]
Methotrexate	ORR 58%, CR 41% in erythrodermic MF[17] ORR 33%, CR 12% in plaque-stage MF[18]
Brentuximab vedotin	ORR 65%, CR 10%[10]
Pralatrexate	ORR 41%, CR <1%[19]
Doxorubicin	ORR 30% to 80%, CR 20% to 60%[20,21]
Gemcitabine	ORR 51.0%–70.5%, CR 11.5%–23.0%[22,23]
Pembrolizumab	ORR 38%, 1 CR[24]
Bortezomib	ORR 67%, CR 17%[25]

Abbreviations: IFN, interferon; ORR, overall response rate.

Table 2: Systemic therapies for mycosis fungoides

Many patients develop resistance against treatments or have relapsing symptoms after a period of improvement. The treatment of relapsed or refractory MF is very challenging due to the limited therapies available [20].

The Cutaneous Lymphocyte Antigen (CLA)

Inflammatory responses are mediated by immune cells that are able to accumulate into tissue sites of inflammation. The migration of leukocytes from the bloodstream to affected tissues is tightly regulated by the interaction between surface molecules expressed on leukocytes and on vascular endothelium [21]. The interference with leukocyte trafficking is included in the effects of established anti-inflammatory drugs, including glucocorticoids [22]. Advancements in the understanding of key immune cell subsets and of their trafficking interactions in inflammatory disorders led to the development of specific inhibitors of leukocyte adhesion molecules. Among targeted therapeutics currently available or in development for the treatment of gastrointestinal and neurologic conditions [23,24], vedolizumab has shown marked clinical efficacy and safety in inflammatory bowel disease without affecting lymphocyte trafficking in the central nervous system and other districts [25]. In the skin, the cutaneous lymphocyte antigen (CLA) is the specific homing receptor for immune cells [26]. Developing a CLA antagonist is an attractive perspective treatment for inflammatory disorders of the skin, where such agent could achieve an analogous role to that of vedolizumab in the gut, combining highly specific effect with excellent safety profile.

The CLA is a carbohydrate surface marker of T-cells that interacts with E-selectin on endothelial cells [27]. Following naive-to-memory transition in skin-draining lymph nodes [28], 15% of circulating T-cells express CLA, which allows migration of memory subsets to inflamed skin, where over 90% of infiltrating T-cells express CLA [29,30]. NK cells, monocytes, granulocytes and a small percentage of memory B-cells also express CLA [31–35], that plays an important role in their skin-homing functions [36]. In the skin, CLA mediates the initial rolling phase of T-cell extravasation from blood vessels to tissue by weak interactions with E-selectin, that is expressed on endothelial cells

following activation by proinflammatory cytokines [37]. Selectins tether the leukocytes exposing them to chemokines and other local stimuli [38]. Chemokines activate integrins, including lymphocyte function-associated antigen 1 (LFA-1) subunit on T-cell surface, which provide for firm adhesion by anchoring to immunoglobulin superfamily molecules, such as intercellular adhesion molecule 1 (ICAM-1) on endothelial cells in the skin [39,40] (Figure 2).
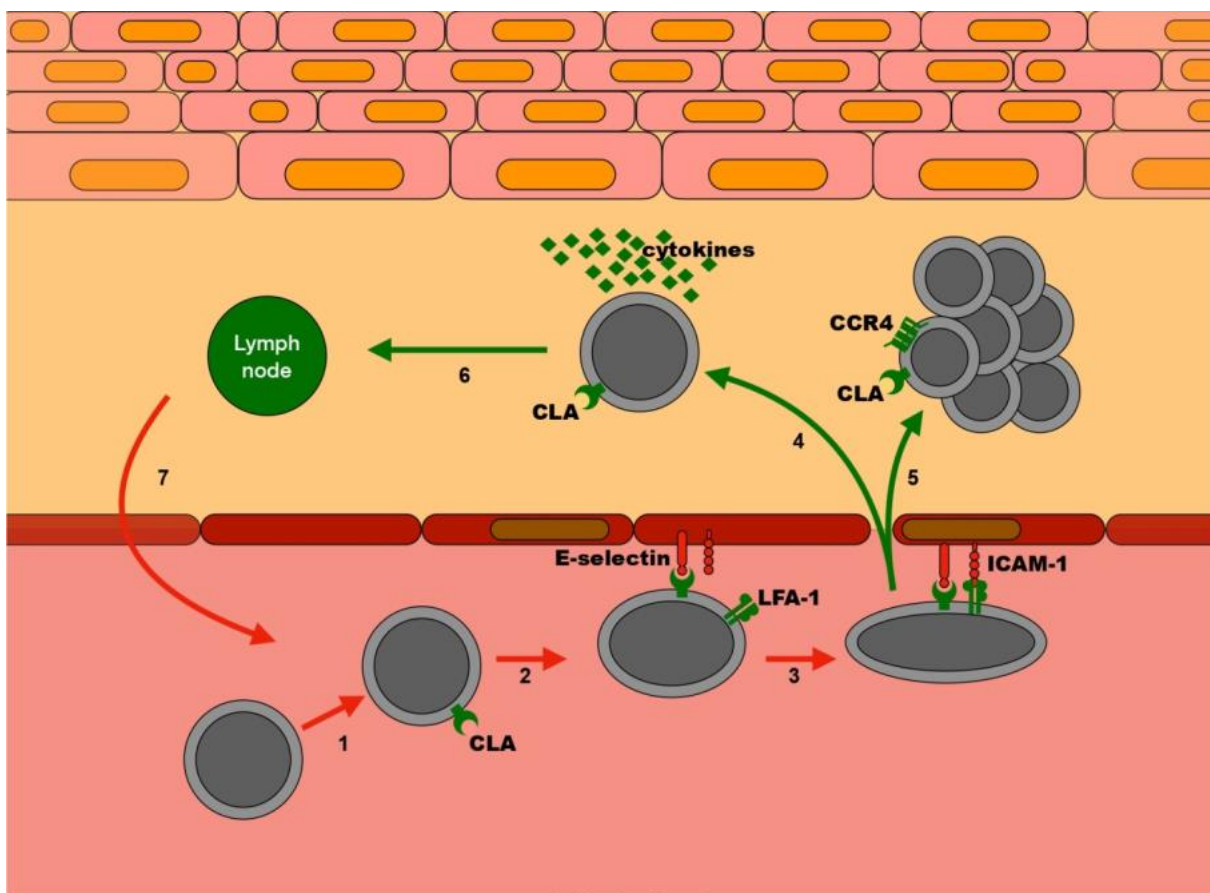

Figure 2. Skin-homing mechanisms of CLA+ T-cells.

CLA is absent on naive T-cells and is expressed following naive-to-memory transition (1). Extravasation of memory T-cells from blood vessels to the skin is dependent on a complex process of rolling and adhesion. The rolling phase is mediated by interaction of CLA on Tcells with E-selectin on endothelial cells (2). The subsequent anchoring phase is mediated by LFA-1 on T-cells and ICAM-1 on the endothelium (3). Effector memory T-cells acquire an activated phenotype responsible for pathogenic cytokine production in inflammatory conditions (4). Malignant T-cells of CTCL also express CLA and CCR4 and preferentially

migrate to the skin (5). A portion of cutaneous memory T-cells undergo a recirculation phenomenon traveling through lymphatics (6) and back to the bloodstream (7). CCR4, CC chemokine receptor type 4; CLA, cutaneous lymphocyte antigen; CTCL, cutaneous T-cell lymphoma ICAM, intercellular adhesion molecule 1; LFA-1, lymphocyte function-associated antigen 1.

In mycosis fungoides (MF), which is the most common form of CTCL, malignant T-cells derive from skin-resident effector memory T-cells [10, 41, 42]. MF lacks the lymph node homing molecules chemokine receptor type 7 (CCR7) and L-selectin, and the differentiation marker CD27 [10]. Conversely, CCR4 and CLA are strongly expressed, resembling the immunophenotype of skin-homing resident effector memory T-cells [10, 41, 42]. Skin-homing resident effector memory T cells usually migrate and stay permanently in the skin without recirculating in the blood flow or entering lymph nodes. Consequently, malignant T-cells in MF remain in skin lesions and account for their long persistence at particular anatomic sites without blood involvement. Magro et al. [9] reported the complete loss of CLA expression in deep dermal and subcutaneous T-cells in the tumor phase MF, while Lu et al. [43] did not describe a difference in CLA expression between skin lesions from early MF (patch and plaque stages) and those from advanced MF (tumor-stage). Furthermore, in parallel with MF progression, malignant T-cells downregulate skin-specific molecules and express lymph node homing molecules [44, 45]. This explains the acquired capacity of these cells to leave the skin and circulate in the bloodstream leading to visceral metastases and/or leukemic involvement.

The expression of CLA is a prognostic factor in CTCL [9]. In particular, the percentage of CLA+ circulating malignant T-cells seems to correlate with the extent of skin symptoms in SS [46, 47]. Expression of CLA has been reported not only in MF and SS, but also in rarer CTCL, such as chronic smoldering variants of adult T-cell lymphoma/leukemia, primary cutaneous epidermotropic CD8+ cytotoxic T-cell lymphoma and CD30+ lymphoproliferative disorders (lymphomatoid papulosis and primary cutaneous anaplastic large cell lymphoma) [9]. While in MF high CLA levels seem to be a

positive prognostic factor corresponding to limited extracutaneous dissemination, CLA expression is not always associated with an indolent clinical course. In NK-like T-cell lymphomas the expression of CLA by NK cells has been correlated with a more aggressive clinical course [48]. Novel molecular targets for the treatment of MF include CLA and CCR4 [49, 50]. CCR4 has a crucial role in the skin-homing of T-cells and is expressed on the surface of malignant Tcells. CCR4 is also involved in the skin trafficking of Th2 and T-reg lymphocytes making it a potential target even for T-cell mediated immune disorders [51]. Mogamulizumab is a fully humanized anti-CCR4 monoclonal antibody approved for the treatment of patients with CTCL who have received at least one prior systemic therapy and is the only agent targeting T-cell skin-homing currently available in this setting [52]. CLA may represent an additional future target for antibody-based therapy because its expression is relatively specific for skin-homing T-cells including malignant cells of CTCL.

Our research focus on developing an anti-CLA antibody-based approach for the treatment of MF.

Near infrared photoimmunotherapy (NIR-PIT)

Near-Infrared Photoimmunotherapy (NIR-PIT) is a novel molecularly targeted phototherapy.

Compared to conventional approaches, NIR-PIT is proving to be a more selective form of treatment. The benefit of using a molecularly targeted phototherapy is that it is able to induce cell death upon NIR radiation only in cells expressing a tumor-specific antigen. Moreover, NIR radiation has proven to be harmless to healthy cells and only penetrates a few centimeters into the skin, thus leaving healthy cells unscathed. [53]

This technique is based on a conjugate of a near-infrared photo-inducible molecule (antibody-photon absorber conjugate, APC) and a monoclonal antibody that targets a tumor-specific antigen. The APC of choice that is currently being used in most experiments and clinical trials is IRDye® 700DX (IR700), a near-infrared, water-soluble, silicon-phthalocyanine derivative.

Cell death is consequently induced through the excitation of the antibody-bound-APC via NIR light at 690 nm [54].

The exact mechanism through which cancer-cell killing is initiated is not fully understood. The most promising theory is that of axial ligand-releasing reaction, as described by Sato et al. [55] Exposure to NIR light causes the APC to release its $C_{14}H_{34}NO_{10}S_3Si$ axial ligand. This chemical reaction, in turn, causes IR700 to become highly hydrophobic and to lose its fluorescence, thus changing the conjugate's shape and solubility in aqueous solutions. The APC's stereoscopic modification causes physical stress and disruption of the cell membrane, leading to the disruption of the transmembrane osmotic gradient (Figure 3). As a result, cells begin to swell, form blebs and burst within only a few minutes of NIR light exposure (Figure 4). [56, 57]
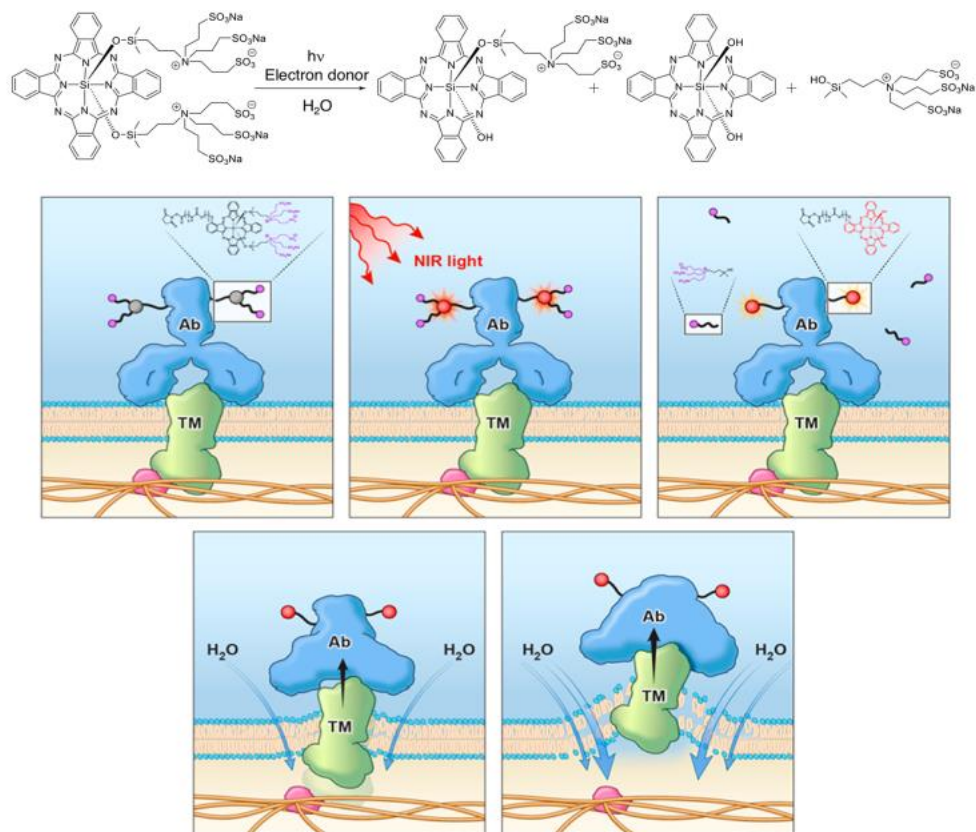
Figure 3: Scheme for chemistry basis of NIR-PIT (top), physical changes conjugated proteins (bottom).
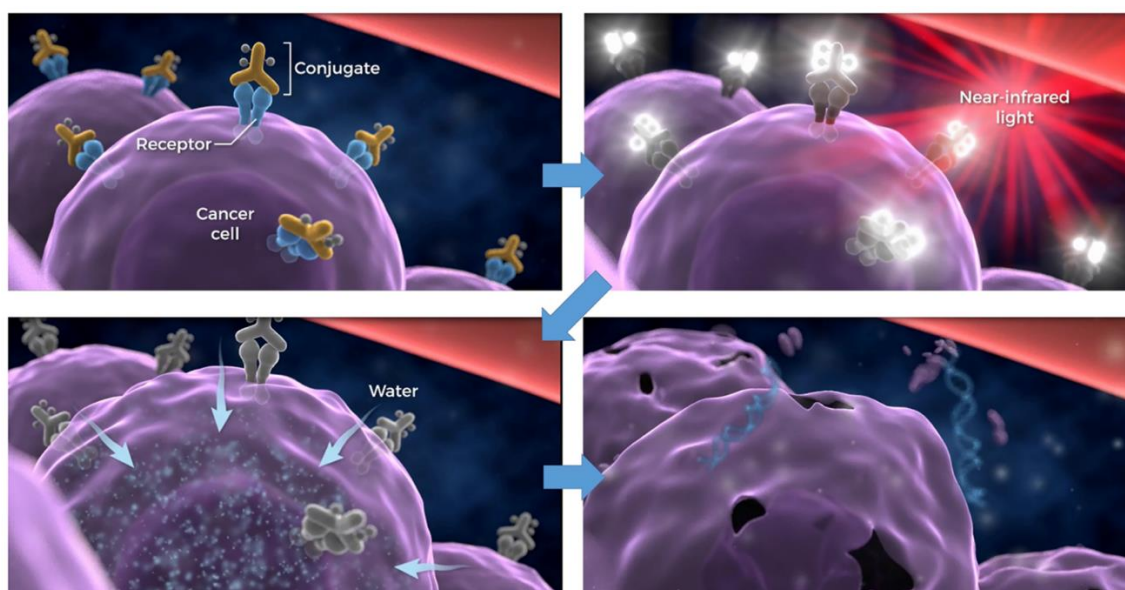

Figure 4: scheme of cellular cytotoxicity induced by NIR-PIT.

This uncontrolled and rapid cell death activates a robust tumor-specific polyclonal immune response. NIR-PIT-treated cancer cells release damage-associated molecular patterns (DAMPs) such as heat shock protein 70 and 90, calreticulin, ATP and HMGB1 in the extracellular space, which are then able to induce local immature dendritic cell (DC) activation. In turn, these now mature DCs prime and educate naïve T cells to become tumor-specific CD8+ T cells inducing immunogenic cell death (ICD) in targeted cancer cells (Figura 5). [58]
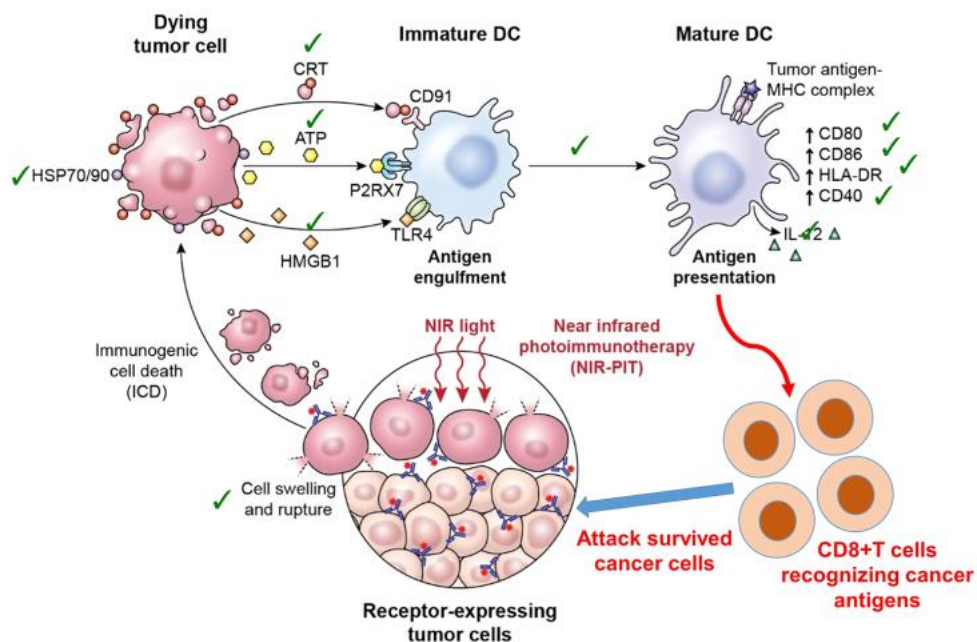

Figure 5: Biology of immunogenic cell death induced by NIR-PIT that leads to enhance antitumor host immunity against treated cancer cells.

The main advantage of NIR-PIT therapy is its low toxicity to healthy tissues. NIR light is a non-ionizing form of radiation that is not damaging to healthy cells, causes no damage to DNA and penetrates only a few centimeters into the tissue. Moreover, the combination of IR700 and a monoclonal antibody results in highly targeted cancer therapy: the APC mainly binds tumor cells that

overexpress the tumor-associated antigen and photoactivation induces death in cancer cells without damaging the adjacent healthy ones. In addition, IR700 is a water-soluble dye with no biotoxic or phototoxic properties of its own; therefore, non-conjugated IR700 that dissociates from the APC is completely harmless and is excreted in urine. [53]

The low toxicity of treatments with NIR-PIT allows to carry out more sessions to eliminate any cancer cells that survived the first treatment. The need for repeated administration could also be reduced by the development of the polyclonal immune response capable of eliminating the remaining tumor cells. Studies have in fact shown that the antitumor host immune-response is enhanced following NIR-PIT thanks to the re-education and proliferation of CD8 + T cells, without any systemic side effects. Therefore, NIR-PIT may lead to the complete eradication of the neoplastic mass after only one or two treatments. [54]

Additionally, NIR-PIT could be combined with conventional immunotherapy, such as checkpoint-inhibitors. This association would enhance its effectiveness by further promoting the activation of CD8 + T cells. Interestingly, the immune systems of laboratory mice in which the tumor mass had been eliminated by combination therapy rejected any attempt to re-inoculate the same neoplastic cells. This would seem to suggest that it is possible to develop immunity against the initial tumor. [59] For this reason, even though NIR-PIT is a local treatment, the induced immune activation is potentially systemic, hence providing a greater-than-expected impact for a 'local' therapy. [53]

The combination of an APC with high target selectivity and the limited exposure of the tumor to NIR rays, therefore, makes NIR-PIT an anticancer therapy with very high specificity and very low toxicity for healthy tissues.

NIR-PIT has demonstrated therapeutic potential for the treatment of solid tumors in several preclinical feasibility mouse studies. [60] Since NIR radiation can only penetrate up to 1 cm deep, the exposure of internal organ tumors may be performed using optical fibers inserted through needle-catheters [61] or endoscopes. [62]

NIR-PIT can be applied to any cancer with overexpressed target membrane proteins for which there is a suitable monoclonal antibody.

To date, this novel approach has been successfully applied to various tumors, which are summarized in Table 3. [63-81]

Cancer type	APCs target
Bladder cancer	EGFR
Bladder cancer	CD47
Prostate cancer	PMSA
Pancreatic cancer	CEA
Liver cancer	GP3C
Gastric peritoneal carcinomatosis	HER2
Colorectal tumors	GPA33
Non-Small-Cell lung cancer and lung metastasis	HER2
Papillary adenocarcinoma of the lung	PD-L1
Lung cancer expressing human EGFR	EGFR
Oral Cavity Squamous Cell Carcinoma	CD44
Disseminated peritoneal ovarian cancer	HER2
Triple-negative breast cancer	EGFR
Triple-negative breast cancer	CD44
Breast cancer	HER2
Glioblastoma	AC133/ CD133
Glioblastoma	EGFR

Table 3: Types of cancer and respective antibody-photon absorber conjugate (APCs) targets for which NIR-PIT has been investigated.

Antibody-drug conjugates (ADCs)

Antibody–drug conjugates (ADCs) are targeted agents that link a cytotoxic drug (also called as cytotoxic payload or warhead) via a linker to a monoclonal antibody which specifically recognizes a cellular surface antigen and deliver toxic payload at the tumor site, thus improving the efficacy of chemotherapy and reducing systemic exposure and toxicity [82].

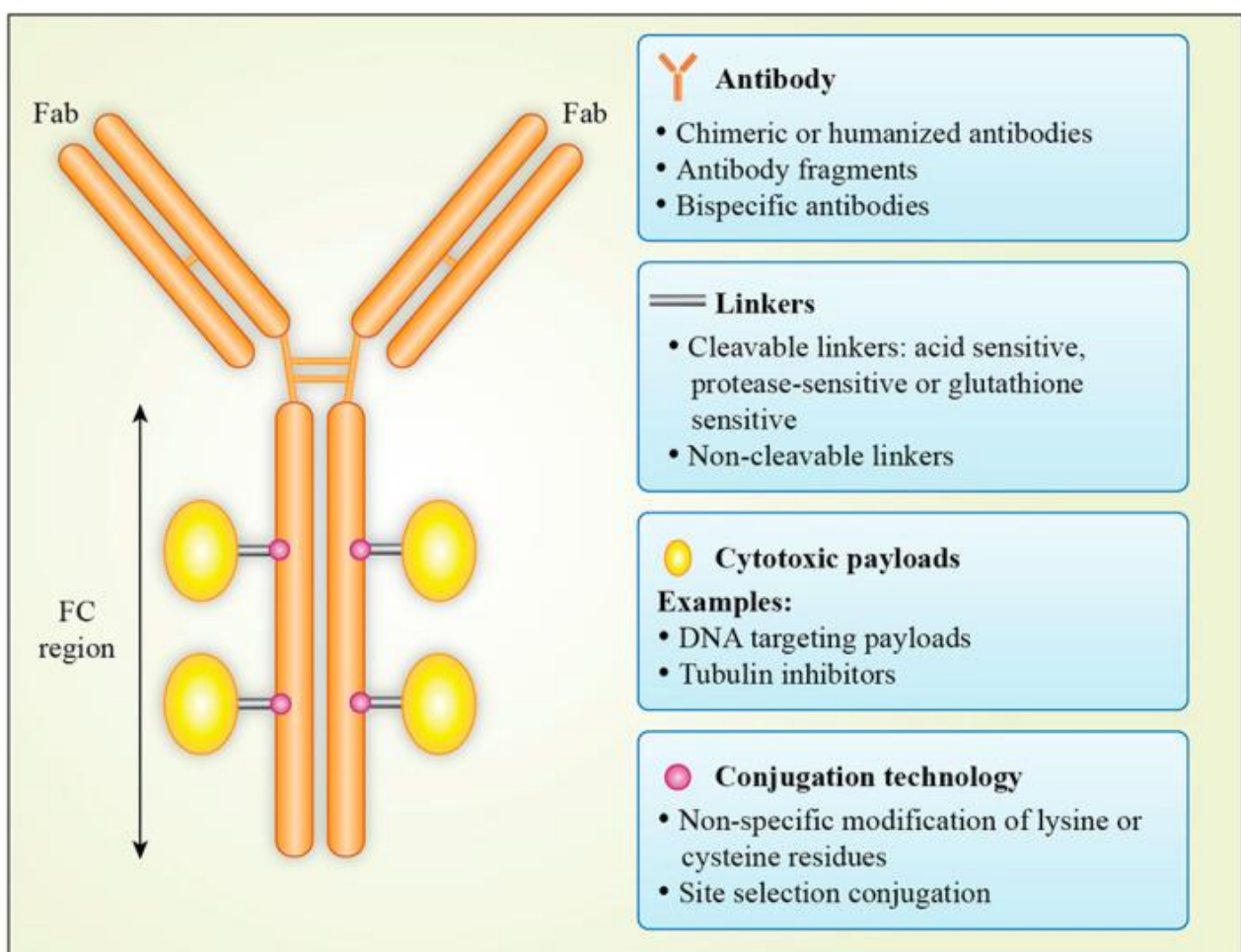More than 80 ADCs are currently under clinical development worldwide [83].

Figure 6: Antibody–drug conjugate structure.

Antibodies incorporated into ADCs are mainly humanized antibodies, significantly less immunogenic than murine and chimeric monoclonal antibodies (mAb). Most of them are based on the IgG1 isotype [84].

Linkers are biochemical compounds connecting the antibody to the payload. Effective linkers have to guarantee ADC stability in the bloodstream as well as to allow an efficient cleavage upon internalization into tumor cells. Linkers can be classified into cleavable and non-cleavable according to their chemical properties [84]. Non-cleavable linkers consist of stable bonds resistant to proteolytic degradation, so that cleavage occurs only after lysosome internalization and complete degradation of the antibody. These linkers have higher stability than cleavable ones, but can suffer from lower membrane permeability.

Most of cytotoxic payloads developed belong to two major families: tubulin inhibitors (maytansinoids or auristatins) and DNA-damaging agents (mainly calicheamicins) [85]. All of them are extremely potent cytotoxic drugs characterized by an IC50 (the inhibitory concentrations that inhibited 50% of cells) in the nanomolar and picomolar range, and an unfavorable toxicity profile if administered systemically [83].

Anti-microtubules agents represent the large majority of warheads developed so far, mainly because of their favorable biochemical properties.

Monomethyl auristatin E (MMAE, vedotin) is a very potent antimitotic agent that inhibits cell division by blocking the polymerisation of tubulin. The family of auristatins are synthetic analogues of the antineoplastic natural product Dolastatin 10 (Figure 7), ultrapotent cytotoxic microtubule inhibitors that are clinically used as payloads in antibody-drug conjugates. [86] Monomethyl auristatin E or MMAE is 100-1000 times more potent than doxorubicin (Adriamycin/Rubex) and cannot be used as a drug itself.

However, as part of an antibody-drug conjugate or ADC, MMAE is linked to a monoclonal antibody (mAb) that recognizes a specific marker expression in cancer cells and directs MMAE to a specific, targeted cancer cell.

The linker linking MMAE to the monoclonal antibody is stable in extracellular fluid, but is cleaved by cathepsin once the antibody-drug-conjugate has bound to the targeted cancer cell antigen and entered the cancer cell, after which the ADC releases the toxic MMAE and activates the potent anti-mitotic mechanism. Antibody-drug conjugates enhance the antitumor effects of antibodies and reduce adverse systemic effects of highly potent cytotoxic agents.
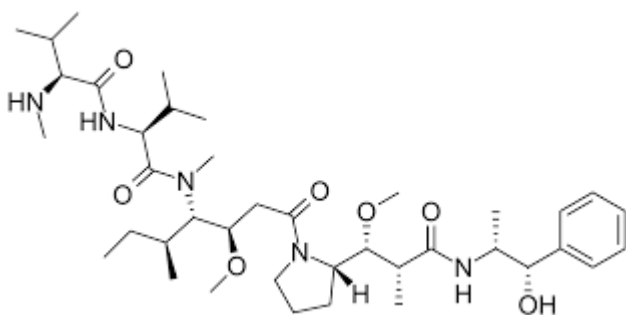

Figure 7: chemical structure of MMAE

Objectives

The aim of the whole PhD project was to investigate novel therapeutic approaches targeting the cutaneous lymphocyte antigen (CLA) for the treatment of mycosis fungoides.

Specific aims were:

1) To investigate the anti-tumor effect of CLA-targeted Near-infrared photoimmunotherapy (NIR-PIT) on MF cells

2) To investigate the anti-tumor effect of the antibody-drug conjugate consisting in anti-CLA monoclonal antibody attached to Monomethyl auristatin E (MMAE) on MF cells

A further aim was to develop a new *in vivo* model of mycosis fungoides by introducing, through xenografting, human MF cells into zebrafish embryos.

1) **To investigate the anti-tumor effect of CLA-targeted Near-infrared photoimmunotherapy (NIR-PIT) on MF**

Methods

Cell culture

The mycosis fungoides cell line used for this study is called MyLa CD4+, purchased from the Sigma-Aldrich company (Catalogue No 95051032). It consists of T cells originating from a skin biopsy of a 82-year-old Caucasian patient affected by stage II mycosis fungoides, with serology negative for HTLV-1. MyLa CD4+ cells express CLA, CD2, CD3, CD4, CD25, CD71, HLA-DR, TCR ß-18 and TCR-1 α/ß.

Cells were cultured in RPMI 1640 medium (Sigma-Aldrich R0883) supplemented with 10% fetal bovine serum (Gibco), 2 mM L-glutamine (G7513), 100 U/L of penicillin and 20U/L of streptomycin.

MyLa CD4+ cells were then grown in a humidified incubator at a temperature of 37°C in an atmosphere saturated with water at a concentration of CO_2 equal to 5%.

Cell viability was evaluated by labeling with a solution of Trypan Blue 0.4% (a life exclusion dye) and subsequent count via the Invitrogen CountessTM Automated Cell Counter hemocytometry chamber.

Conjugation of anti-CLA antibody to IRDye® 700DX

For the experiments, the anti-CLA antibody was conjugated to the IRDye® 700DX.

The anti-CLA antibody used is the "CLA Antibody, anti-human, PE, REAfinityTM", clone REA 1101, purchased from the company Miltenyi Biotec (catalogue no. 130119043). It is a recombinant IgG1 monoclonal antibody.

For the conjugation of IRDye®700DX protein we used the conjugation kit purchased from the LiCor company (catalogue number 92838046). It contains IRDye® 700DX, a photostable silicon phthalocyanine with chemical formula $C_{74}H_{96}N_{12}Na_4O_{27}S_6Si_3$; it should be stored at -20°C in the absence of light.

LED Lamp

The lamp used for irradiation, MIC-LED-690M (Prizmatix Ltd., Israel) (Figure 8), is based on a single chip LED (Light Emitting Diode) at high power with a built-in adjustable aspherical lens collimator with anti-reflection coating. Specifically, this NIR light emitting diode emits with a peak at 695 nm and a centroid at 687 nm, with a FWHM (Full Width at Half Maximum) of 25 nm (Figure 9). The collimated power, i.e. the power of the total beam emitted by the LED head after passing the collimating aspherical lens internally, is 210 mW.
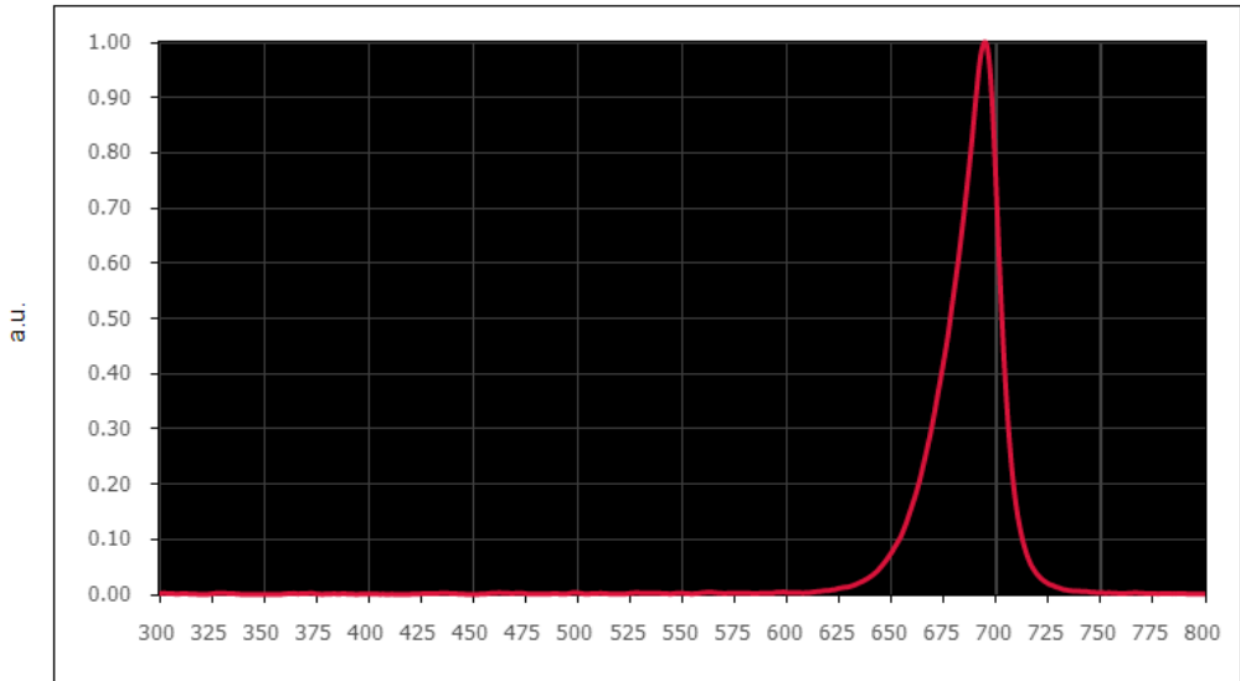
Figure 8. MIC-LED-690M (https://www.prizmatix.com/MicLED/Mic-LEDs.aspx)

Figure 9: Peak emission of the MIC-LED-690M (https://www.prizmatix.com/MicLED/Mic-LEDs.aspx)

The collimator allows to obtain a uniform distribution on the surface of wells (diameter = 20 mm) containing the cells. The irradiation obtained was of about 0.05 W/cm2.

In vitro CLA-targeted NIR-PIT

Cells in suspension were plated (600,000 cells/ml) in medium Complete RPMI 1640 in 24-well plates (Figure 10). Initially, we performed preliminary experiments with various amount of antibody in order to find the most effective dose. To check the specificity of the treatment, cells treated with anti-

CLA-IR700 but without irradiation and cells irradiated but not incubated with the antibody were used as a negative control.
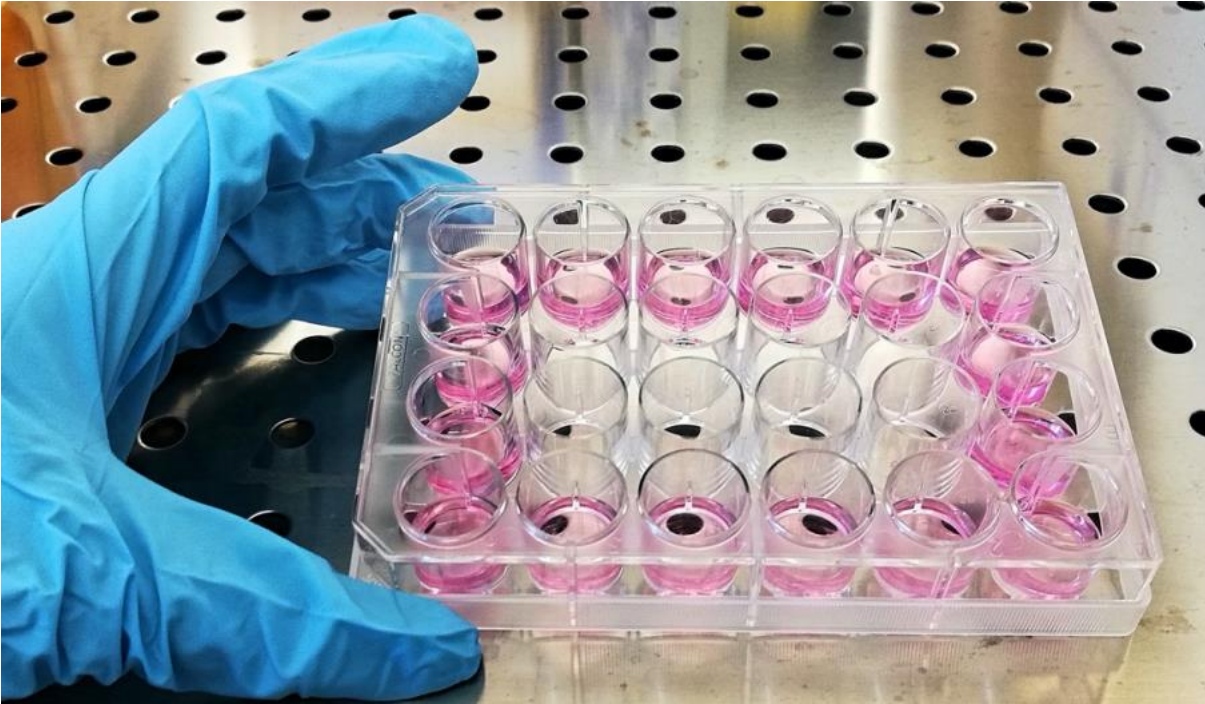

Figure 10. MyLa CD4+ cells in suspension.

The cells were treated with 5 µg of anti-CLA-IR700 conjugate (diluted in 5 µL) and incubated for 30 minutes at 37°C, then cells were exposed to infrared radiation for 5 minutes (Figure 11). After 24 h levels of cell death were analyzed.
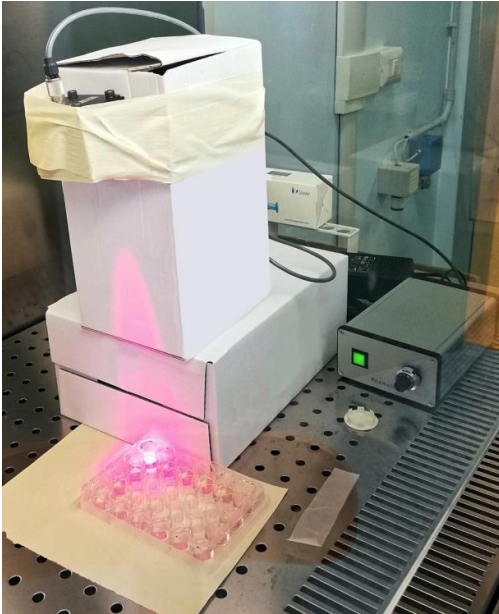
Figure 11. Irradiation of MyLa CD4+ cells treated with anti-CLA-IR700 by MIC-LED-690M.

Flow cytometry and cell death assay

Flow cytometry is a laboratory technique that uses a beam of laser light for detection, counting, characterization and separation of cells in suspension. This technique makes use of the flow cytometer, an instrument capable of measuring different morphological parameters at the same time resulting from the crossing of single cells by the laser light beam.

Specific fluorophores can be used as markers. Each fluorophore has a specific excitation and emission wavelength. After 24 hours from the treatment, cells were labeled with 2 µg/ml of iodide of propidium (PI) in RPMI1640 medium for 10 minutes at room temperature ed analyzed with BDTM LSR II Flow Cytometer-Becton Dickinson, equipped with 4 lasers (405, 488, 563, 646 nm).

Propidium is a fluorescent intercalator of DNA, which is excluded by vital cells thanks to the activity of the MDR pumps (Multidrug resistance pumps) present on cells membrane; consequently, only permeabilized or dead cells will be positive.

Culture and treatment of MyLa CD4+ cells in VitroGel®

Since the tumor microenvironment is essential for mycosis fungoides cells, VitroGel® (The Well Bioscience) which is a three-dimensional culture model mimicking the extracellular matrix was used to confirm in vitro efficacy of anti-CLA NIR-PIT (Figure 12). Vitrogel® is a hydrogel unmodified polysaccharide with adjustable mechanical properties, stable at room temperature, pH neutral, transparent, permeable and compatible with different imaging systems.

The VitroGel® was diluted with water for injections (B. Braun) in a 1:3 ratio and MyLa CD4+ cells (7.5×10^5 cells/ml) in a 2:1 ratio. 600 µL of the cell and VitroGel® solution were then plated in a 24-well plate and incubated for 10-20 minutes at room temperature. At the end of the gelling process, 1 mL of RPMI 1640 medium was added to complete each well. The cells were maintained in culture for 48 h in an incubator temperature of 37°C in an atmosphere saturated with water and at a concentration of CO_2 equal to 5%. The cells were then incubated with anti-CLA-IR700 antibody and irradiated as described above.
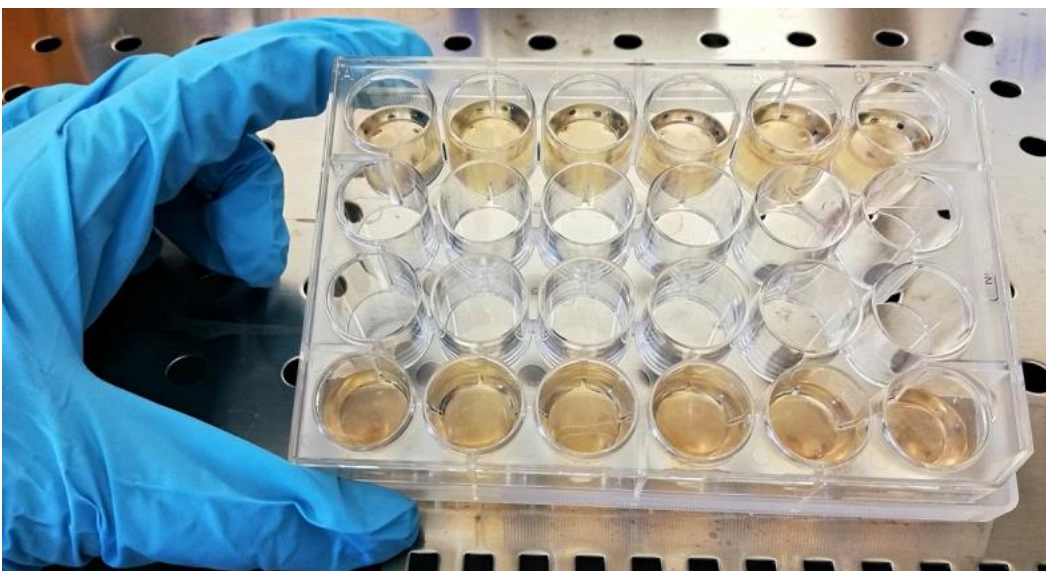

Figure 12: MyLa CD4+ cells in VitroGel®

ROS production analysis

In order to evaluate the possible production of reactive oxygen species (ROS), levels of lipid peroxidation in MyLa CD4+ cells were measured 24 hours after treatment with the anti-CLA-IR700 antibody.

Lipid peroxidation refers to the oxidative degradation of cell lipids by the ROS. The peroxidation of unsaturated lipids alters the properties cell membrane and signal transduction pathways. Besides, it is usually present in drug-induced phototoxicity processes.

The Image-iT® Lipid Peroxidation Kit is based on the BODIPY® reagent 581⁄591 C11, a fluorescent reagent that changes the emission wavelength from 590 nm to 510 nm when oxidized. The samples were labeled with 5 µM of ImageiT® Lipid Peroxidation Sensor directly in the culture medium for 30 minutes.

Analysis was made using LSRII flow cytometry (BD).

Statistical analysis

The statistical analysis and graphs have been carried out using SigmaPlot version 13.0 software (Systat Software, Inc., San Jose, CA,USA). Statistical analysis were performed using the nonparametric test of the Mann-Whitney rank sum. Results that yielded p-values <0.05 (*), <0.01 (**), <0.001 (***) were considered statistically significant.

Results

Treatment with CLA-targeted NIR-PIT induces cell death in MyLa cells

Previous studies conducted at the Istituto Oncologico Veneto (IOV) and Unit of Dermatology have shown that 90% of MyLa CD4+ cells express the CLA antigen (Figure 13). These data were further confirmed using confocal microscopy, by which it was possible to demonstrate that CLA has a prevalent distribution at the plasma membrane (Figure 14).
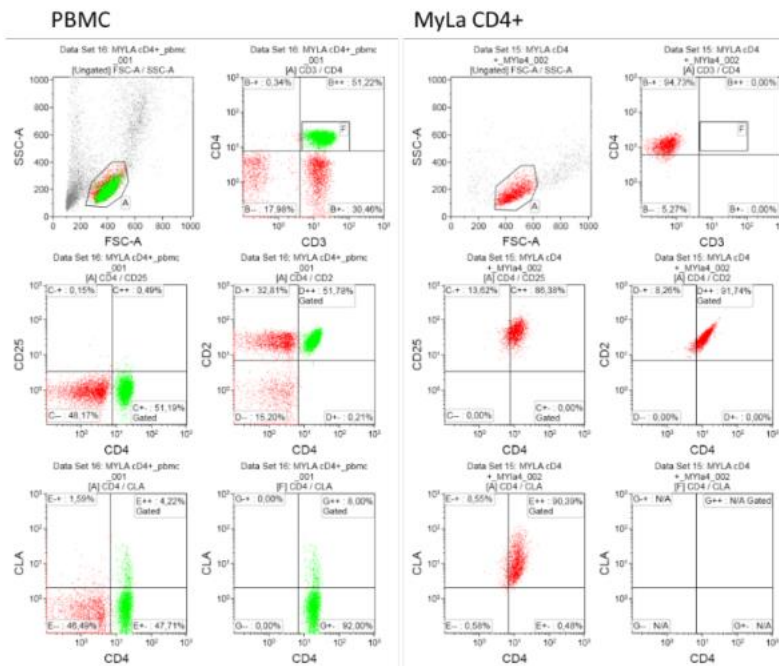

Figure 13: Immunophenotypic characterization of MyLa CD4+ cells and PBMCs from healthy donors.

Cells were labeled with CD2, CD3, CD4, CD25, CLA and analyzed by LSRII BD flow cytometer.
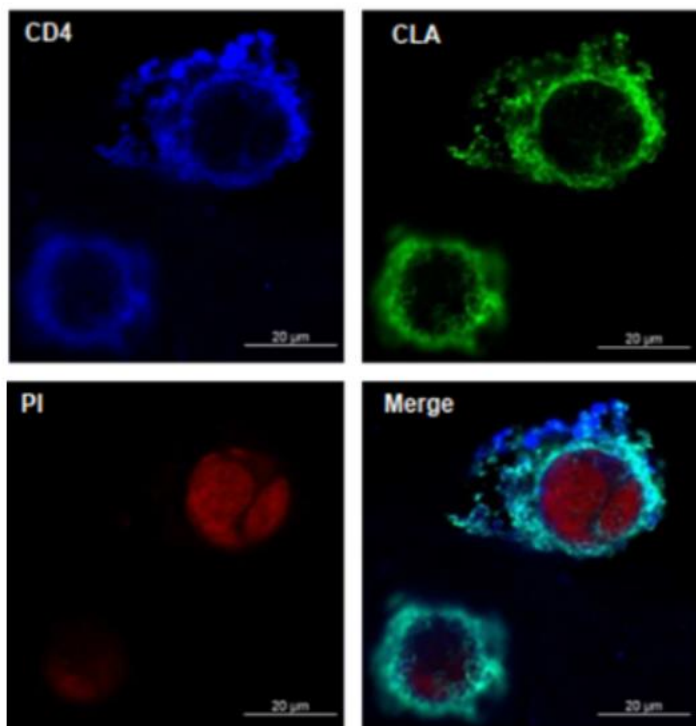
Figure 14: My-La CD4+ cells stained with anti-CD4 antibodies (blue), anti-CLA antibodies (green), and propidium iodide to identify nuclei (red). Images were obtained with a confocal microscope Zaiss LS510 using a 63X objective and a digital zoom of 3.

Therefore, CLA could be a potential molecular target for MF. An anti-CLA monoclonal antibody-based approach may be a novel and highly selective treatment for MF. In particular a CLA-targeted near infrared photoimmunotherapy (NIR-PIT) would confer significant therapeutic advantages, such as high selectivity, the reduction of side effects and reduction of the risk of systemic immunosuppression.

We have successfully combined the pure anti-CLA antibody to the photoinducible molecule IRDye® 700DX. Figure 15 shows the peaks corresponding to the fluorescence of Myla CD4+ cells labeled with anti-CLA monoclonal antibody conjugated with IR700 (green peak) and MyLa CD4+ labeled with pure anti-CLA monoclonal antibody (red peak) used as controls.
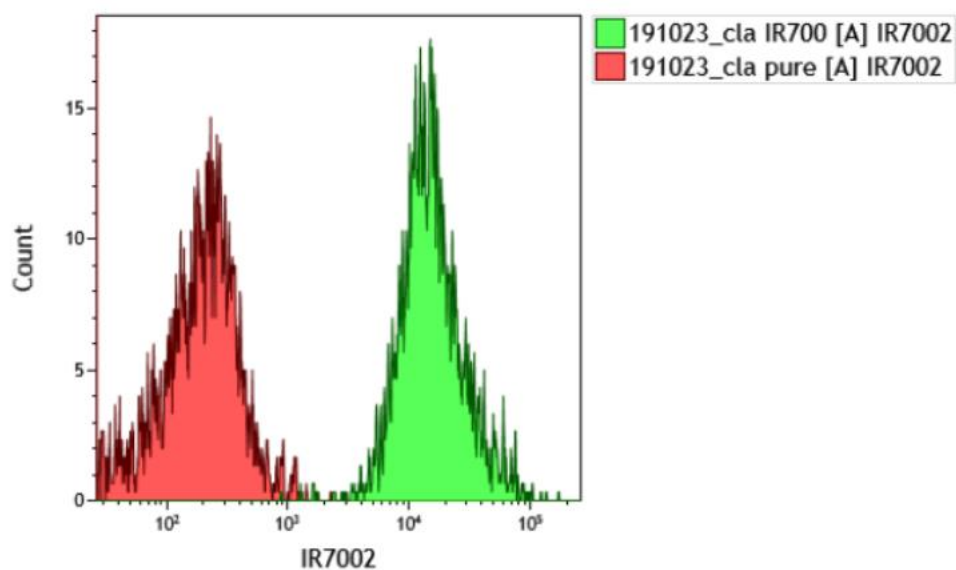
Figure 15: Flow cytometric analysis of anti-CLA antibody. The analysis has been performed using a LSRII flow cytometer, BD, equipped with 405-nm, 488-nm, 560-nm and 647-nm lasers. The emission signals were detected with 720/45 nm bandpass filters.

MyLa-CD4+ cell were treated for 24 h with increasing concentrations of unconjugated anti-CLA monoclonal antibody demonstrating that the antibody itself does not influence cell death (Figure 16). In order to validate NIR-PIT *in vitro*, MyLa CD4+ cells were treated with anti-CLA monoclonal antibody conjugated to IR700 and then irradiated with a NIR light emitting diode with peak of emission at 695 nm. Preliminary experiments in which the amount of conjugate was varied have shown that the percentage of dead cells following treatment increases as the amount of conjugate increases. Figure 16 shows the curve representing the percentage of cells death given by the increase of the conjugate, with an irradiation time equal to 5 minutes.
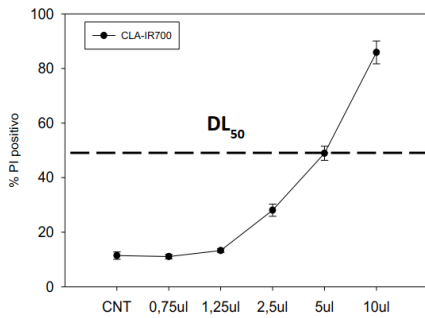
Figure 16: Increase in the percentage of dead cells given by the increase of added conjugate. The percentage of cells death was evaluated counting propidium iodide-positive cells.

For the final validation of CLA-targeted NIR-PIT we used the amount of conjugate corresponding to the lethal dose 50 (LD50 = 5 µL, with concentration 1 µg/µL). Results of these experiments are summarized in Figure 17. Treatment with anti-CLA or NIR light irradiation alone exhibited very modest pro-death effects, while the combination of the two induced a substantial increase in death in the MF cell line. The difference was statistically significant ($p = 0.008$).

Data obtained demonstrate that CLA-targeted NIR-PIT has a marked anti-tumor effect *in* vitro on MF cells.
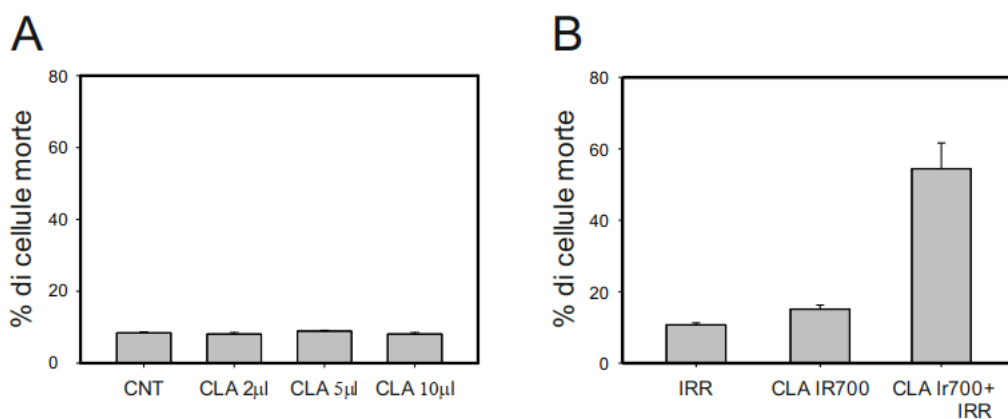
Figure 17: Levels of death of MyLa-CD4+ cells treated for 24 h with increasing concentrations of unconjugated anti-CLA antibody (A) Death levels of irradiated MyLa-CD4+ cells, treated with the anti-CLA antibody conjugated to IR700 and the combination of two treatments (B). Experiments were performed in triplicate, with $p = 0.008$.

IRDye® 700DX-anti-CLA and NIR induce the increase in ROS

To evaluate whether treatment with the CLA-targeted NIR-PIT causes an increase in ROS production, level of lipid peroxidation has been evaluated in samples treated with anti-CLA-IR700 conjugate and irradiated with infrared light and compared to controls treated with NIR irradiation alone or the conjugate alone. Data obtained suggest that CLA-targeted NIR-PIT causes an increase in ROS production (Figure 18).

Lipid peroxidation

Figure 18: Evaluation of lipid peroxidation levels in the samples treated with the antiCLA-IR700 conjugate and irradiated with infrared light and in the controls treated with the irradiation alone or with the conjugate alone.

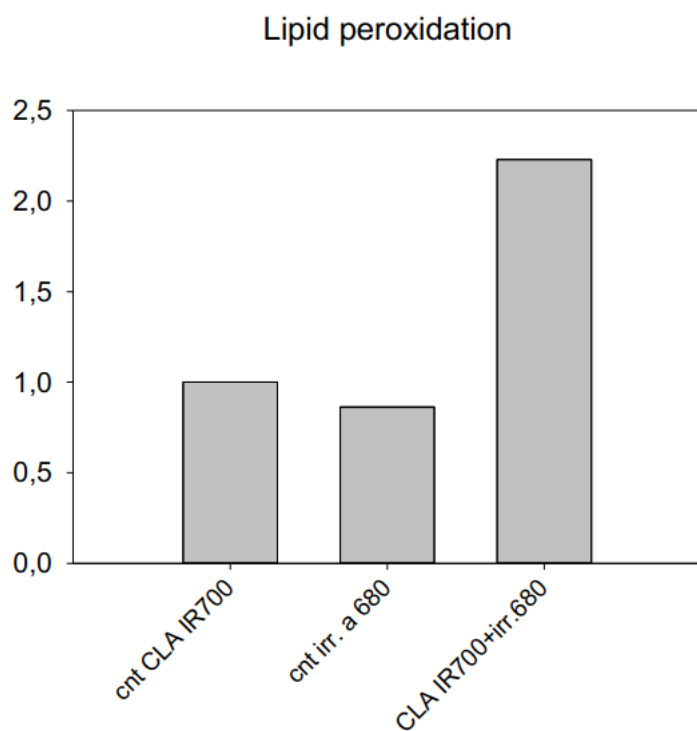**2) To investigate the anti-tumor effect of the antibody-drug conjugate consisting in anti-CLA monoclonal antibody attached to Monomethyl auristatin E (MMAE) on MF cells**

Methods

Cell culture

In order to test new possible therapeutic strategies for the treatment of MF *in vitro*, we used the cell line called MyLa CD4+ (Merck, Catalog No. 95051033), originally derived from the skin biopsy of a patient affected by plaque-phase MF, with negative serology for HTLV-1.

Patient-derived immortalized cancer cell lines, although hard to establish, are easy to use, and provide primary platforms for evaluating molecular pathways associated with malignant transformation and identification of cancer cell intrinsic vulnerabilities for drug screening purposes. CTCL cells have been studied extensively to explore their genomic and transcriptomic similarities among cell lines (as a group), as well as between cell lines and patient samples. We routinely culture many T-lineage cell lines in RPMI 1640 medium (Euroclone) supplemented with 10% fetal bovine serum (FBS, Sial), 2 mM L-glutamine L glutamine, 100U/L penicillin and 20U/L streptomycin ('RPMI'). As the data sheet supplied with the MyLa CD4+ cells indicated that their culture medium requires supplementation with human serum and cytokines (IL-2 and IL-4), we initially cultured them with these additional components, and then gradually adapted them to growth in RPMI. The adapted cell line is herein referred to as 'MyLa'. MyLa cells grow in suspension forming characteristic cellular aggregates, which indicate good viability.

The ideal seeding concentration is between 300,000 and 900,000 cells/ml and was determined by setting up cultures at different concentrations. Cell viability was evaluated by labelling cells with

0.4% Trypan Blue, a vital exclusion dye which, by entering cells that have lost the integrity of the cytoplasmic membrane, stains only dead cells, discriminating them from live cells. MyLa cells were grown in a humidified tissue culture incubator, at a temperature of 37°C, in a water-saturated, 5% CO2 atmosphere.

Conjugation of anti-CLA monoclonal antibody with MMAE

Monomethyl auristatin E (MMAE) was conjugated to CLA antibody (Mal-VC-PAB-MMAE) using a kit from CellMosaic Inc. (Woburn, MA, USA) following the manufacturer's instructions (Figure 19).

Description of the Material:
(a) **Chemical Name**: IgMk-VC-PAB-MMAE
(b) **Project Number**: 5404
(c) **Starting Material Source 1**: CLA Antibody from Miltenyi Biotec, Cat# 130-092-629, Lot# 5220505662
(d) **Starting Material Source 2**: Mal-VC-PAB-MMAE from CellMosaic. Stock#: CM11001, Lot#: s396.s3.0330B
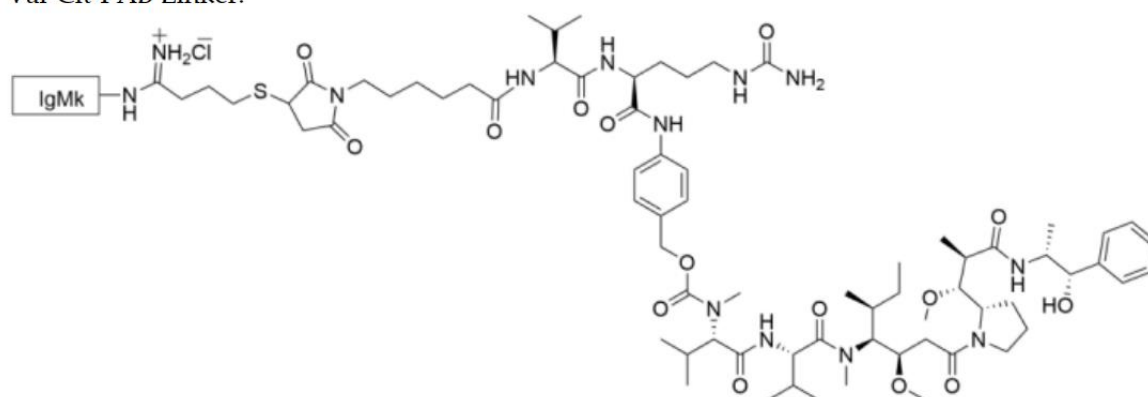(e) **Conjugation chemistry**: Antibody IgMk and MMAE are linked together via releasable Val-Cit-PAB Linker.

Figure 19: anti-CLA monoclonal antibody and MMAE linked together via releasable Val-Cit-PAB Linker.

Flow cytometry

Flow cytometry is a technique that allows to quantify different parameters (morphology, expression of specific molecules detected by fluorescent antibodies/probes) in a suspension of cells. The flow cytometer consists of 4 main components: (1) a fluidic component, which transports the cells to them counting chamber; (2) a series of lasers, whose beams are crossed by cells; (3) photomultipliers, which detect the optical signal and convert it into an electrical signal; and (4) data-processing software. Flow cytometry permits analysis of individual cells in a sample in a very short time (seconds).

Cell death assay

After 24h of treatment with the single compounds or with their combinations, aliquots of cells were labeled with 2 μg/ml propidium iodide (PI) and 2 μl annexin V conjugated to the Alexa 647 fluorophore (Thermo Fisher Scientific) in 300 μl RPMI medium for 10 min at room temperature, and then analyzed by flow cytometry. PI is a chemical compound capable of penetrating exclusively into cells that have a damaged cell membrane, then binding stoichiometrically to the nuclear DNA. Annexin V, on the other hand, binds to phosphatidylserine, which is exposed on the outer surface of the cell membrane of apoptotic cells.

Live cells are both PI- and Annexin V-negative, early apoptotic cells are Annexin V-positive and PInegative, while both Annexin V and PI positivity indicate late apoptosis. Necrotic cells are positive for PI only. The specific cell death reported in the figures was calculated with the following formula: $SCD = [(CDT - CDNT)/(100-CDNT)] \times 100$ where CDT indicates the percentage of dead cells in treated samples, and CDNT indicates the percentage of dead cells in control samples.

Immunoblotting

SDS-polyacrylamide gel electrophoresis-immunoblotting is a standard technique that permits sizedependent separation of proteins in complex lysates and their identification/quantification using specific antibodies after transfer to a membrane support. After treatments described in the text, aliquots of cells were collected, washed with PBS, and then lysed in cell disruption buffer (Ambion) containing inhibitors of phosphatases and proteases (PhosphoSTOP and Complete, Roche). Proteins were separated by SDS/PAGE in 4–20% Tris-HEPES gradient gels (BioRad) and transferred onto nitrocellulose membranes (GE Healthcare). The membranes were saturated with 3% bovine serum albumin prepared in TBS (50 mM TRIS-Cl, pH 7.5, 150 mM NaCl)-0.01% Tween-20, and then incubated overnight with mouse anti-G6PD antibody (Santa Cruz Biotechnology, 1:1000) and rabbit anti-GAPDH antibody (GeneTex International Corp., 1:10000). Membranes were then washed twice and incubated for 1h with horseradish peroxidase (HRP)-conjugated anti-mouse and anti-rabbit antibodies (Thermo Fisher Scientific, 1:5000). Chemiluminescent signals were detected using Lite Ablot Turbo (EuroClone) and a Cambridge UVITEC imaging system.

Statistical analyses and preparation of figures

Statistical significance was evaluated using the nonparametric Mann-Whitney rank sum test calculated with SigmaPlot version 13.0 software (Systat Software, Inc.). Statistical significance was considered at $p<0.05$. Graphs were generated using Sigmaplot version 13.0. Figures were prepared using Powerpoint.

Results

Cell death induced by MMAE and MMAE+ Anti-CLA-Ab treatment

Most cytotoxic drugs used in cancer pharmacotherapy do not preferentially localize at the tumor site, causing undesired toxicities that restrict dose increases. This problem can be overcome by attaching the drug to a molecule that will selectively bind to and be taken up by the tumor cells. MMAE (monomethyl auristatin E) is an anti-mitotic agent which inhibits cell division by blocking the polymerization of tubulin. We attempted to make MMAE cytotoxicity specific for MF cells by conjugating it to a monoclonal antibody (ab) recognizing Cutaneous Lymphocyte Antigen (CLA), a characteristic homing receptor expressed by MF cells (See Figure 1.1). In order to evaluate the ability of the antibody-drug conjugate (ADC) to induce cell death, MyLa cells were treated with MMAE, CLA-ab, or ADC (ab-MMAE) at the concentrations indicated in Figure 20. Results showed that MMAE was able to induce death in MyLa cells in a dose-dependent manner (Figure 20A, left-hand panel). However, the ADC exhibited lower cytotoxic activity compared to MMAE or CLA-ab alone (Figure 20B, right-hand panel).
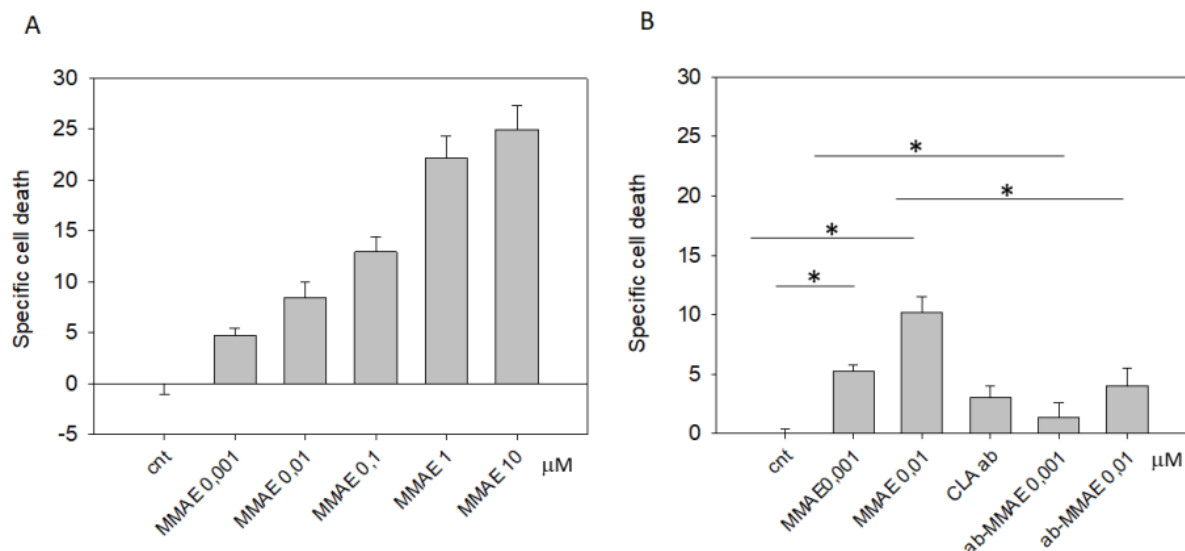
Figure 20: **Treatment of MyLa cells with MMAE and ab-MMAE.** The left-hand panel (A) shows death of MyLa cells, calculated as specific cell death, after 24h of treatment with increasing doses of MMAE (indicated in µM). The right-hand panel (B) shows death induced by MMAE and CLA-ab used as single agents, compared to the ADC (ab-MMAE). Statistically significant differences between the control cells and the cells treated with MMAE or ab-MMAE were calculated using the non-parametric Mann-Whitney test.

Detection of CLA and CLA-MMAE on/in MyLa cells

The low cytotoxic activity observed for ab-MMAE prompted us to verify whether the MyLa cells were bound by the ADC and internalized it. To this end, we incubated MyLa cells with vehicle, CLAab, or ab-MMAE for 72 hours. Cells were then washed and, without fixing or permeabilizing them, incubated with FITC-conjugated secondary antibody and analyzed by flow cytometry. As shown in Figure 21, the percentages of FITC-positive cells were higher in both the CLA-ab treated sample (80.8%) and the ab-MMAE treated sample (62.7%) compared to the untreated control (1.83%). This result indicated that the ab-MMAE conjugate bound to the cell surface but perhaps was not efficiently internalized into the cells.
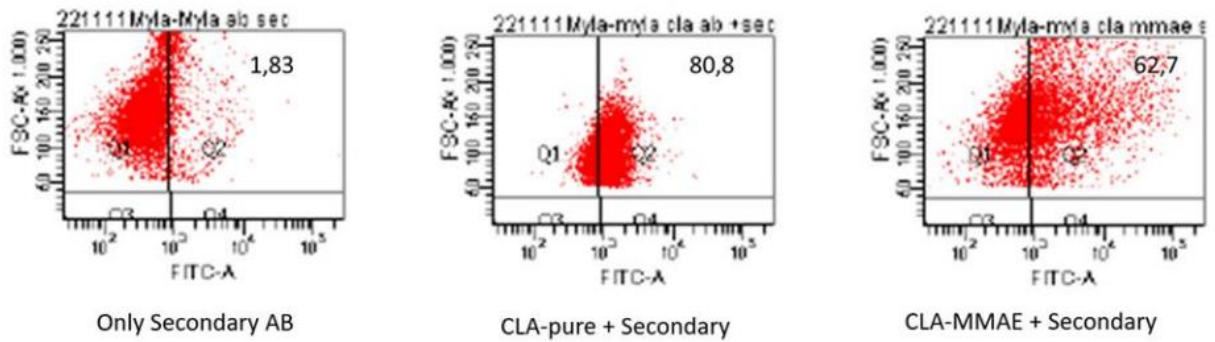
Figure 21: Detection of CLA and CLA-MMAE on MyLa cells. MyLa cells were cultured for 72h with CLA-ab and ab-MMAE and then labelled with the FITC-conjugated secondary antibody for 1h at RT. CLApositive cells were detected by flow cytometry.

3) **To develop a zebrafish embryo model of mycosis fungoides**

Methods

Transfection of mycosis fungoides cells

The mycosis fungoides cell line named MyLa CD4+, purchased from Sigma-Aldrich (catalog number 95051032) has been used for this study.

The zebrafish belonged to the mutant strain casper (mitfa w2 / mpv17 a9 alleles, according to the ZFIN database) which has the characteristic of maintaining transparency even in the adult individuals.

To make tumor cells detectable and well differentiated from those of the zebrafish embryo, MyLa CD4+ mycosis fungoides cells were transfected with an exogenous plasmid containing GFP (Green Fluorescent protein).

The pMax-GFP DNA plasmid, specially made for eukaryotic expression, was purchased by the biotech company Amaxa, Lonza Group AG brand.

The technique used for the transfection of the plasmid was electroporation consisting in an electric discharge which increases the permeability of the plasma membrane facilitating the entry of plasmid in the cytoplasma and then in the nucleus where it will be transcribed.

The cells, once transfected, were placed in a culture medium and in a second time analyzed to observe the expression of GFP by microscopy and cytofluorimetry.

Xenotransplantation

Zebrafish embryos were obtained from the mating of casper adults. Specifically, on day 0 (mating day) eggs were harvested and incubated at 28 C in Fish Water (Embryo Medium: 0.33 mM CaCl2•2H2O, 0.33 mM MgSO4•7H2O, 0.1% Methylene blue in distilled water). At day 2 post-fertilization (2 dpf) the embryos were deprived of the chorion by mechanical removal, using insulin needles.

To perform the transplant, the 2 dpf embryos were anesthetized with Tricaine (MS222; E10521, Sigma–Aldrich, Milan, Italy), used at 0.16 mg/mL in Fish Water. The anesthetized embryos were aligned along a multi-lane plastic support, immersed in a medium consisting of 2% methyl cellulose in PBS (137 mM NaCl, 2.7 mM KCl, 4.3 mM Na2HPO4, 1.47 mM KH2PO4, pH 7.4). The MyLa cells, prepared to the final density of 0.2 x 106 cells/uL, were loaded into a vitreous capillary needle, then connected to a pressure microinjector (WPI PicoPump apparatus). Through micro-injections, the cells were deposited in the center of the yolk of each embryo (about 100-200 cells per embryo). Finally, the embryos were collected, resuscitated and incubated in new Fish Water, keeping them at 33°C, a compromise temperature between 28°C of zebrafish and 37°C of human cells.

Subdivision into different groups and lots

For the purposes of the study, zebrafish two days post-fertilization (day post fertilization, dpf) were divided into two groups and their mortality was evaluated for four consecutive days. The control group, i.e. the one in which no transplant was performed, was composed of four batches, for a total of 85 embryos; the transplanted group was also composed of four lots, for a total of 61 embryos. Furthermore, of the 4 lots transplanted, three of these (for a total of 48 embryos) were transplanted with 100-200 MyLa cells, while the fourth batch (for a total of 13 embryos) was transplanted with <10 MyLa cells.

Image acquisition

Once the cellular transplant has been carried out, to verify the goodness of the precedent processes, the embryos were analyzed by fluorescence microscopy. To acquire images, the larvae were anesthetized with Tricaine and photographed with a Leica M165FC dissecting microscope, equipped with a Leica DFC7000T CCD camera controlled by Leica Application software Suite (LAS V4.8,

Leica Microsystems, Wetzlar, Germany). The panels of images were assembled with Adobe Photoshop 21.1.1.

Quantification of signals

The acquired signals were quantified using the "Measurements" option of the Volocity 6.0 software (Perkin Elmer, Milan, Italy). Pairwise statistical analysis between groups of measurements was performed by Unpaired t-test, while the comparisons between multiple groups of measurements were performed with ANOVA, followed by Tukey test (Graph Pad Prism V7.0 software).

Histological analyses

Transplanted zebrafish surviving at 6 dpf were fixed in paraformaldehyde 4% (PFA) in Phosphate Buffered Saline (PBS) at 4C for issue preservation and subsequent histological investigations.

Ethical approval

The experiments with zebrafish were carried out in accordance with Italian and European legislation (Directive 2010/63/EU) and with permission for animal testing released by the Ethics Committee of the University of Padua (OPBA) and by Italian Ministry of Health (Authorisation n. 407/2015-PR).

Results

A small batch of embryonic zebrafish was transplanted 2 days post-fertilization (2 dpf) and viewed 24 hours later, at 3 dpf /1 dpi (1 day post injection), using a dissecting microscope, equipped with a camera. An example of an embryo transplanted is shown in Figure 22, where it is possible to note the mass cell transplanted into the yolk region, both in visible light and in fluorescent light.
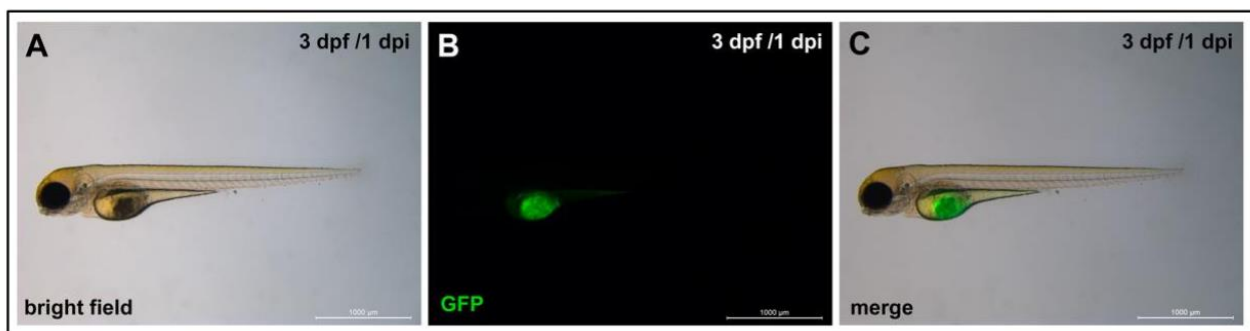
Figure 22: Example of a zebrafish embryo at 3 dpf/1 dpi, harboring a cell mass transplanted into the region of the yolk. The cell mass is observable *in vivo* in bright field (A, bright field), under green fluorescent light (B, GFP) and superimposed signals (C, merge); green fluorescence is emitted by GFP produced by transfected cells. All images are in lateral, anterior view to the left.

146 zebrafish used in the study were first divided into two groups, the xenotransplant group and the control one. Examples of controls e xenografts, observed at 1 dpi (3 dpf) and at 4 dpi (6 dpf), are illustrated in Figure 23.
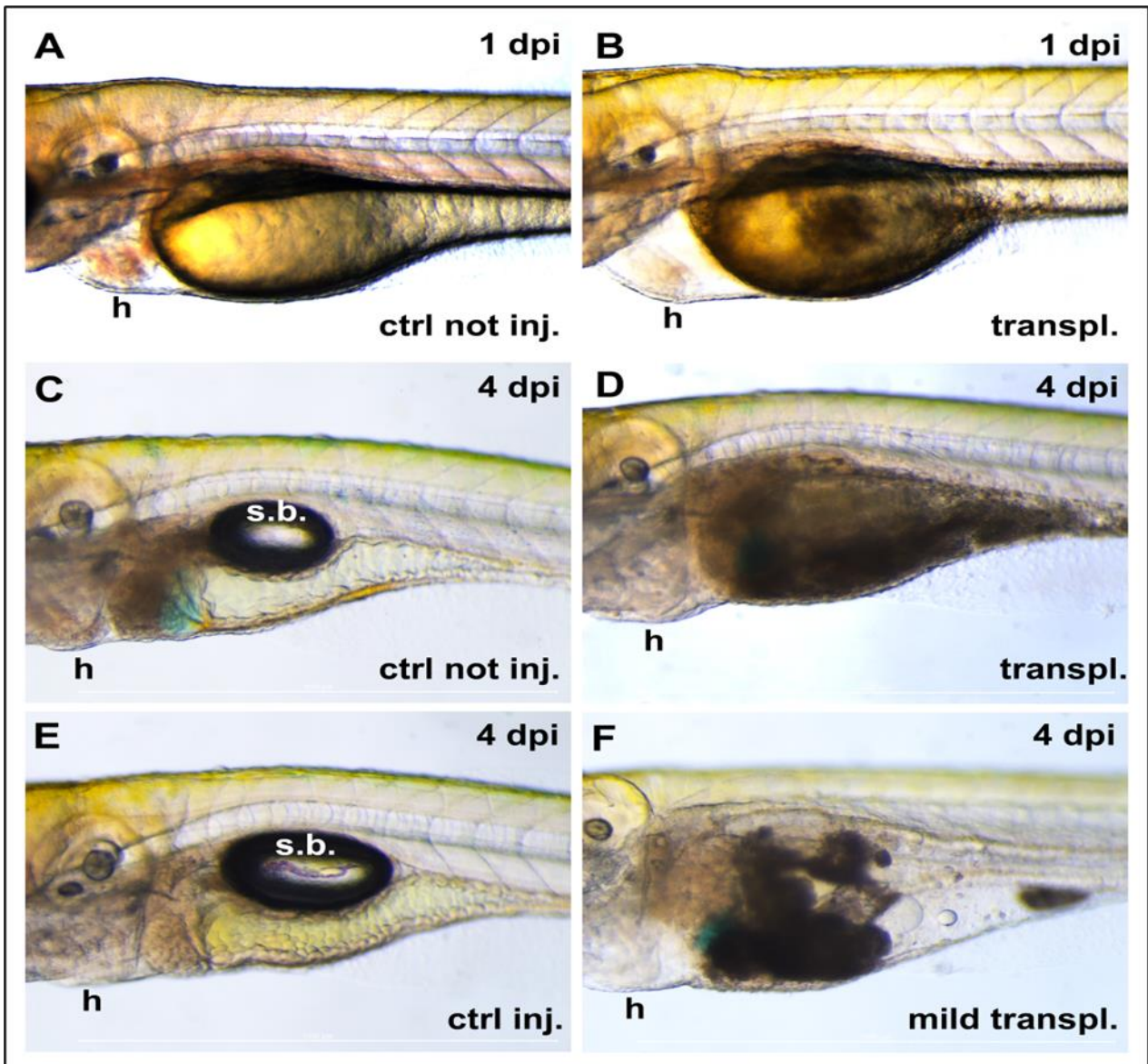
Figure 23: Xenotransplantation of mycosis fungoides cells in zebrafish and monitoring over time. (TO) Control embryo at the 3 dpf stage, not transplanted, observed at 1 dpi (day post injection). (B) Transplanted embryo, analyzed at 1 dpi. Note the cell mass deposited in the center of the yolk. (C) Control, uninjected larva observed at 4 dpi (6 dpf). Note the presence of the swim bladder (sb: swim bladder). (D) Transplanted larva: note the invasion of the entire area of the yolk from the transplanted cells. The swim bladder is absent. (E) Control larva injected with control solution (cell medium); the appearance is indistinguishable from a non larva injected. (F) Injected larva with few cells. Despite the limited number of cells of departure, there is appreciable invasion of the yolk area. The swim bladder is absent. In all images the heart is indicated by h (heart). Note the tendency to pericardial edema in transplanted zebrafish. All images are side view, front left.

Subsequently, a further division into 4 subgroups was performed.

In the non-transplant control group, consisting of 85 zebrafish, mortality at 6dpf was 4.7%.

The xenotransplantation group consisted of 61 embryos of which 48 (belonging to batches 1-2-3) were injected with 100-200 tumor cells, while the 13 embryos belonging to batch 4 were transplanted with <10 tumor cells. In the first three batches at 6dpf (4dpi) mortality was 91.7%, while in batch 4 mortality was 38.5%. In the 8 zebrafish of this lot alive at 6 dpf histological analysis demonstrated the presence of large tumor masses in 50% of them and the presence of tumor cells in 87.5% of the embryos.

The xenotransplantation experiments performed to evaluate the proliferation of mycosis fungoides cells in zebrafish embryos have given very positive and extremely encouraging results, confirming the possible use of this animal species as a model for the study of this pathology.

Discussion:

There are currently few effective therapies for the treatment of MF, which must take into consideration skin extension, staging, relapse, patient age and any comorbidities. Treatments for the early stages generally consist of a skin-directed therapy, and treatments for the late stages are generally systemic, and often combined. Although the initial stages of MF have usually a moderate clinical course, 30% of patients relapse or prove to be refractory to currently used treatments and are destined to progress to advanced stages of the disease for which, in fact, there is not a curative treatment. There is no evidence that more aggressive therapies (notably polychemotherapy) prolong survival. Furthermore, in advanced stages therapies rarely provide long-lasting responses and the only potential curative therapy is allogenic hematopoietic stem-cell transplantation for which not all patients will be eligible because of its high treatment-related morbidity and mortality rates.

Novel molecular targets for the treatment of MF include CLA and CCR4 [87, 88]. CCR4 has a crucial role in the skin-homing of T-cells and is expressed on the surface of malignant Tcells. CCR4 is also involved in the skin trafficking of Th2 and T-reg lymphocytes making it a potential target even for T-cell mediated immune disorders [89]. Mogamulizumab is a humanized monoclonal antibody with a defucosylated Fc region that targets and inhibits CCR4. By binding to the N-terminal domain of CCR4, mogamulizumab causes antibody-dependent cellular cytotoxicity [90]. Also, by depleting CCR4-positive regulatory T-cells, it is thought that mogamulizumab can enhance the host immune system's antitumor activity. Mogamulizumab has been approved for the treatment of patients with CTCL who have received at least one prior systemic therapy and is the only agent targeting T-cell skin-homing currently available in this setting [90]. Mogamulizumab demonstrated significant improvement in progression-free survival compared with vorinostat in patients with relapsed or refractory MF. Serious adverse events associated with mogamulizumab include infusion-related reactions, cutaneous drug eruption, and autoimmune complications. Mogamulizumab administration

in the preallogeneic hematopoietic stem cell transplant setting can increase the risk for severe posttransplant graft-versus-host disease [91].

In the skin, CLA is the specific homing receptor for immune cells. CLA is a carbohydrate surface marker of T-cells that interacts with E-selectin on endothelial cells. CLA is strongly expressed by MF tumor cells and it could be another specific molecular target for the treatment of MF. An anti-CLA monoclonal antibody-based approach may represent a novel and highly selective treatment for this disease.

The aim of this PhD project was to investigate novel therapeutic approaches targeting CLA for the treatment of MF. Two different anti-CLA monoconal antibody-based approaches have been evaluated *in vitro*.

The first approach consisting in CLA-targeted NIR-PIT showed marked anti-tumor effect *in vitro* which is indicative of the translation potential of this approach. NIR-PIT offers several advantages over conventional cancer treatments, and it is ideal for surface-located skin cancers. Targeted-NIR-PIT is a high selective therapy with virtually no damage to normal adjacent structures. Furthermore, it exploits a form of non-ionising radiation and for this reason no limits to its total cumulative dose have been reported, and multiple cycles of NIR-PIT could be safely employed. CLA-targeted NIR-PIT should be validated in an *in vivo* system because it seems to be a really promising treatment for MF.

The second approach consisting in an anti-CLA monoclonal antibody conjugated to MMAE demonstrated a low cytotoxic activity *in vitro*. The low cytotoxic activity observed for this ADC prompted us to verify whether MyLa cells were bound by the ADC. To this end, we incubated MyLa cells with vehicle, anti-CLA alone or anti-CLA-MMAE conjugate for 72 hours. Cells were then washed and, without fixing or permeabilizing them, incubated with FITC-conjugated secondary antibody and analyzed by flow cytometry indicating that the anti-CLA-MMAE conjugate binds the cell surface. Probably the low cytotoxicity activity could be explained by the lack of internalization

of the ADC into the cells *in vitro*. However, it has recently been demonstrated that *in vivo* non-internalizing antibodies may have potent anti-cancer activity thanks to proteolytic release of MMAE in the subendothelial extracellular matrix [92]. Thus, although its low anti-tumor activity *in vitro*, with think that anti-CLA-MMAE conjugate may be effective *in vivo*.

Although CLA is promising target for MF therapy, it should be remind that not all MF tumor cells express CLA and its expression seems to decrease during disease progression and this could be a limit of CLA-targeted approaches. However, it has been recently reported that monoclonal antibody therapy may have a potent anti-tumor effect also if not all tumor cells express the monoclonal antibody target. For example, if only10% of tumor cells are CD30 positive, this is sufficient for brentuximab vedotin to elicit a therapeutic response [93].

A further limit of CLA-targeted approaches depends on whether CLA is expressed also by healthy T cells normally residing in the skin. It can therefore be assumed that the use of an anti-CLA monoclonal antibody-based approach can lead to a number of side effects resulting from an alteration of the skin immune system. At the same time, while CLA is expressed also by T cells involved in inflammatory skin disorders, developing a CLA antagonist is an attractive perspective treatment also for these diseases.

The first future goal of this research project is to evaluate the efficacy of CLA-targeted NIR-PIT in an adequate three-dimensional model as culture of MyLa CD4+ cells in VitroGel® in the presence of normal keratinocytes and fibroblasts or the more complex T-Skin TM/Reconstructed Human Full-Thickness Skin Model (EPIskin). The second future goal consists in performing *in vivo* phase studies in order to evaluate the anti-tumor effect of these new approaches in an animal model of MF.

Recently, the zebrafish has been established as one of the most important model organisms for medical research. Several studies have proved that there is a high level of similarity between human and zebrafish genomes, which encourages the use of zebrafish as a model for understanding human genetic disorders, including cancer. Interestingly, zebrafish skin shows several similarities to human

skin, suggesting that this model organism is particularly suitable for the study of neoplastic and inflammatory skin disorders.

The xenotransplantation experiments performed to evaluate the proliferation of MF cells in zebrafish embryos have given very positive and extremely encouraging results, confirming the possible use of this animal species as a model for the study of this pathology.

Owing to its low maintenance cost, highly conserved genome, and easy genetic manipulation, zebrafish embryo xenograft is an excellent model for preclinical research in dermatological laboratories, thus bridging the gap between *in vitro* cell culture an in *vivo* mammalian models. *In vivo* validation phases studies are ongoing on zebrafish embryos to investigate the efficacy of these anti-CLA monoclonal antibody-based approaches.

References:

1. Willemze R, Cerroni L, Kempf W, et al. : The 2018 update of the WHO-EORTC classification for primary cutaneous lymphomas. Blood. 2019;133(16):1703–14.

2. Korgavkar K, Xiong M, Weinstock M. Changing incidence trends of cutaneous T-cell lymphoma. JAMA Dermatol 2013;149(11):1295–9.

3. Imam MH, Shenoy PJ, Flowers CR, et al. Incidence and survival patterns of cutaneous T-cell lymphomas in the United States. Leuk Lymphoma 2013;54(4):752–9.

4. Jawed SI, Myskowski PL, Horwitz S, Moskowitz A, Querfeld C. Primary cutaneous Tcell lymphoma (mycosis fungoides and Sézary syndrome): part I. Diagnosis: clinical and histopathologic features and new molecular and biologic markers. J Am Acad Dermatol. 2014 Feb;70(2):205.e1-16.

5. Larocca C, Kupper T. Mycosis Fungoides and Sézary Syndrome: An Update. Hematol Oncol Clin North Am. 2019 Feb;33(1):103-120.

6. Willemze R. Mycosis fungoides variants-clinicopathologic features, differential diagnosis, and treatment. Semin Cutan Med Surg. 2018 Mar;37(1):11-17.

7. Alsayyah A. Is it mycosis fungoides? A comprehensive guide to reaching the diagnosis and avoiding common pitfalls. Ann Diagn Pathol. 2020 Aug;47:151546.

8. Pulitzer MP, Horna P, Almeida J. Sézary syndrome and mycosis fungoides: An overview, including the role of immunophenotyping. Cytometry B Clin Cytom. 2020 Jun 9.doi: 10.1002/cyto.b.21888.

9. Magro CM, Dyrsen ME. Cutaneous lymphocyte antigen expression in benign and neoplastic cutaneous B- and T-cell lymphoid infiltrates. J Cutan Pathol. 2008 Nov;35(11):1040-9.

10. Campbell JJ, Clark RA, Watanabe R, et al. Sezary syndrome and mycosis fungoides arise from distinct T-cell subsets: a biologic rationale for their distinct clinical behaviors. Blood 2010;116(5):767–71.

11. Clark RA, Chong B, Mirchandani N, et al. The vast majority of CLA1 T cells are resident in normal skin. J Immunol 2006;176(7):4431–9.

12. Wang XN, McGovern N, Gunawan M, et al. A three-dimensional atlas of human dermal leukocytes, lymphatics, and blood vessels. J Invest Dermatol 2014; 134(4):965–74.

13. Clark RA. Skin-resident T cells: the ups and downs of on site immunity. J Invest Dermatol 2010;130(2):362–70.

14. Clark RA. Resident memory T cells in human health and disease. Sci Transl Med 2015;7(269):269rv261.

15. Watanabe R, Gehad A, Yang C, et al. Human skin is protected by four functionally and phenotypically discrete populations of resident and recirculating memory T cells. Sci Transl Med 2015;7(279):279ra239.

16. Watanabe R, Teague JE, Fisher DC, et al. Alemtuzumab therapy for leukemic cutaneous T-cell lymphoma: diffuse erythema as a positive predictor of complete remission. JAMA Dermatol 2014;150(7):776–9.

17. Clark RA, Watanabe R, Teague JE, et al. Skin effector memory T cells do not re-circulate and provide immune protection in alemtuzumab-treated CTCL patients. Sci Transl Med 2012;4(117):117ra117.

18. Trautinger F, Eder J, Assaf C, et al. European Organisation for Research and Treatment of Cancer consensus recommendations for the treatment of mycosis fungoides/Sézary syndrome - Update 2017. Eur J Cancer 2017;77:57-74.

19. Nguyen CV, Bohjanen KA. Skin-Directed Therapies in Cutaneous T-Cell Lymphoma. Dermatol Clin 2015;33:683-96.

20. Papadaki M, Saraki K, Karagianni F, et al. Cutaneous T-cell lymphoma: aetiopathogenesis and current diagnostic and therapeutic developments. Eur J Dermatol. 2020 Apr 16. doi: 10.1684/ejd.2020.3712.

21. Nourshargh S, Alon R. Leukocyte migration into inflamed tissues. Immunity. 2014;41:694–707.

22. Nakagawa M, Bondy GP, Waisman D, et al. The effect of glucocorticoids on the expression of L-selectin on polymorphonuclear leukocyte. Blood. 1999;93:2730–2737.

23. Stefanelli T, Malesci A, De La Rue SA, et al. Anti-adhesion molecule therapies in inflammatory bowel disease: touch and go. Autoimmun. Rev. 2008;7:364–369.

24. Polman CH, O'Connor PW, Havrdova E, et al. A randomized, placebo-controlledm trial of natalizumab for relapsing multiple sclerosis. N. Engl. J. Med. 2006;354:899–910.

25. Lobatón T, Vermeire S, Van Assche G, et al. Review article: anti-adhesion therapies for inflammatory bowel disease. Aliment. Pharmacol. Ther. 2014;39:579–594.

26. Santamaria LF, Perez Soler MT, Hauser C, et al. Allergen specificity and endothelial transmigration of T cells in allergic contact dermatitis and atopic dermatitis are associated with the cutaneous lymphocyte antigen. Int. Arch. Allergy Immunol. 1995;107:359–362.

27. Berg EL, Yoshino T, Rott LS, et al. The cutaneous lymphocyte antigen is a skin lymphocyte homing receptor for the vascular lectin endothelial cell-leukocyte adhesion molecule 1. J. Exp. Med. 1991;174:1461–1466.

28. Picker LJ, Treer JR, Ferguson-Darnell B, et al. Control of lymphocyte recirculation in man. II. Differential regulation of the cutaneous lymphocyte-associated antigen, a tissue-selective homing receptor for skin-homing T cells. J. Immunol. 1993;150:1122–1136.

29. Fuhlbrigge RC, Kieffer JD, Armerding D, et al. Cutaneous lymphocyte antigen is a specialized form of PSGL-1 expressed on skin-homing T cells. Nature. 1997;389:978–981.

30. D'Ambrosio D, Iellem A, Colantonio L, et al. Localization of Th-cell subsets in inflammation: differential thresholds for extravasation of Th1 and Th2 cells. Immunol. Today. 2000;21:183–186.

31. Kieffer JD, Fuhlbrigge RC, Armerding D, et al. Neutrophils, monocytes, and dendritic cells express the same specialized form of PSGL-1 as do skin-homing

memory T cells: cutaneous lymphocyte antigen. Biochem. Biophys. Res. Commun. 2001;285:577–587.

32. Tsuchiyama J, Yoshino T, Toba K, et al. Induction and characterization of cutaneous lymphocyte antigen on natural killer cells. Br. J. Haematol. 2002;118:654–662.

33. Chang S-E, Kim M-J, Lee W-S, et al. Natural killer cells in human peripheral blood and primary cutaneous natural killer cell lymphomas may express cutaneous lymphocyte antigen. Acta Derm. Venereol. 2003;83:162–166.

34. Yoshino T, Okano M, Chen HL, et al. Cutaneous lymphocyte antigen is expressed on memory/effector B cells in the peripheral blood and monocytoid B cells in the lymphoid tissues. Cell. Immunol. 1999;197:39–45.

35. Armerding D, Fuhlbrigge RC, Kieffer JD, et al. Tonsillar B cells do not express PSGL-1, but a significant fraction displays the cutaneous lymphocyte antigen and exhibits effective E- and P-selectin ligand activity. Int. Arch. Allergy Immunol. 2001;126:78–90.

36. Kantele A, Savilahti E, Tiimonen H, et al. Cutaneous lymphocyte antigen expression on human effector B cells depends on the site and on the nature of antigen encounter. Eur. J. Immunol. 2003;33:3275–3283.

37. Woodland DL, Kohlmeier JE. Migration, maintenance and recall of memory T cells in peripheral tissues. Nat. Rev. Immunol. 2009;9:153–161.

38. Kishimoto TK, Rothlein R. Integrins, ICAMs, and Selectins: Role and Regulation of Adhesion Molecules in Neutrophil Recruitment to Inflammatory Sites. Adv. Pharmacol. 1994;25:117–169.

39. Thelen M, Stein J V. How chemokines invite leukocytes to dance. Nat. Immunol. 2008;9:953–959.

40. Alon R, Ley K. Cells on the run: shear-regulated integrin activation in leukocyte rolling and arrest on endothelial cells. Curr. Opin. Cell Biol. 2008;20:525–532.

41. Beyer M, Mobs M, Humme D, et al. Pathogenesis of Mycosis fungoides. J. Dtsch. Dermatol. Ges. 2011;9:594–598.

42. Wilcox RA. Cutaneous T-cell lymphoma: 2017 update on diagnosis, riskstratification, and management. Am. J. Hematol. 2017;92:1085–1102.

43. Lu D, Duvic M, Medeiros LJ, et al. The T-cell chemokine receptor CXCR3 is expressed highly in low-grade mycosis fungoides. Am. J. Clin. Pathol. 2001;115:4 421.

44. Ferran M, Romeu ER, Rincon C, et al. Circulating CLA+ T lymphocytes as peripheral cell biomarkers in T-cell-mediated skin diseases. Exp. Dermatol. 2013;22:439–442.

45. Krieg C, Boyman O. The role of chemokines in cancer immune surveillance by the adaptive immune system. Semin. Cancer Biol. 2009;19:76–83.

46. Borowitz MJ, Weidner A, Olsen EA, et al. Abnormalities of circulating T-cell subpopulations in patients with cutaneous T-cell lymphoma: cutaneous lymphocyte-associated antigen expression on T cells correlates with extent of disease. Leukemia. 1993;7:859–863.

47. Heald PW, Yan SL, Edelson RL, et al. Skin-selective lymphocyte homing mechanisms in the pathogenesis of leukemic cutaneous T-cell lymphoma. J. Invest. Dermatol. 1993;101:222–226.

48. Yoshino T, Nakamura S, Suzumiya J, et al. Expression of cutaneous lymphocyte antigen is associated with a poor outcome of nasal-type natural killer-cell lymphoma. Br. J. Haematol. 2002;118:482–487.

49. Welborn M, Duvic M. Antibody-Based Therapies for Cutaneous T-Cell Lymphoma. Am. J. Clin. Dermatol. Springer International Publishing; 2019. p. 115–122.

50. Alaibac M. Monoclonal antibodies against cutaneous T-cell lymphomas. Expert Opin. Biol. Ther. 2017;17:1503–1510.

51. Yoshie O, Matsushima K. CCR4 and its ligands: from bench to bedside. Int. Immunol. 2015;27:11–20.

52. Oka T, Miyagaki T. Novel and Future Therapeutic Drugs for Advanced Mycosis Fungoides and Sezary Syndrome. Front. Med. 2019;6:116.

53. Kobayashi H, Furusawa A, Rosenberg A, Choyke PL. Near-infrared photoimmunotherapy of cancer: a new approach that kills cancer cells and enhances anti-cancer host immunity. *Int Immunol*. 2021;33(1):7-15.

54. Kobayashi H, Choyke PL. Near-Infrared Photoimmunotherapy of Cancer. Acc Chem Res. 2019 Aug 20;52(8):2332-2339.

55. Sato K, Ando K, Okuyama S, et al. Photoinduced Ligand Release from a Silicon Phthalocyanine Dye Conjugated with Monoclonal Antibodies: A Mechanism of Cancer Cell Cytotoxicity after Near-Infrared Photoimmunotherapy. *ACS Cent Sci*. 2018;4(11):1559-1569.

56. Nakamura Y, Nagaya T, Sato K, et al. Alterations of filopodia by near infrared photoimmunotherapy: evaluation with 3D low-coherent quantitative phase microscopy. *Biomed Opt Express*. 2016;7(7):2738-2748.

57. Ogata F, Nagaya T, Okuyama S, et al. Dynamic changes in the cell membrane on three dimensional low coherent quantitative phase microscopy (3D LC-QPM) after treatment with the near infrared photoimmunotherapy. *Oncotarget*. 2017;8(61):104295-104302.

58. Ogawa M, Tomita Y, Nakamura Y, et al. Immunogenic cancer cell death selectively induced by near infrared photoimmunotherapy initiates host tumor immunity. *Oncotarget*. 2017;8(6):10425-10436.

59. Nagaya T, Friedman J, Maruoka Y, et al. Host Immunity Following Near-Infrared Photoimmunotherapy Is Enhanced with PD-1 Checkpoint Blockade to Eradicate Established Antigenic Tumors. *Cancer Immunol Res*. 2019;7(3):401-413. *

The results analyzed in this article demonstrate that the reversal of adaptive immune resistance that follows the use of NIR-PIT results in high rates of tumor rejection and tumor growth control in cancer models.

60. Paraboschi I, Turnock S, Kramer-Marek G, et al. Near-InfraRed PhotoImmunoTherapy (NIR-PIT) for the local control of solid cancers: Challenges and potentials for human applications [published online ahead of print, 2021 Apr 6]. *Crit Rev Oncol Hematol*. 2021;161:103325

61. Okuyama S, Nagaya T, Sato K, et al. Interstitial near-infrared photoimmunotherapy: effective treatment areas and light doses needed for use with fiber optic diffusers. *Oncotarget*. 2018;9(13):11159-11169.

62. Nagaya T, Okuyama S, Ogata F, Maruoka Y, Choyke PL, Kobayashi H. Endoscopic near infrared photoimmunotherapy using a fiber optic diffuser for peritoneal dissemination of gastric cancer. *Cancer Sci*. 2018;109(6):1902-1908.

63. Railkar R, Krane LS, Li QQ, et al. Epidermal Growth Factor Receptor (EGFR)-targeted Photoimmunotherapy (PIT) for the Treatment of EGFR-expressing Bladder Cancer. *Mol Cancer Ther*. 2017;16(10):2201-2214.

64. Kiss B, van den Berg NS, Ertsey R, et al. CD47-Targeted Near-Infrared Photoimmunotherapy for Human Bladder Cancer. *Clin Cancer Res*. 2019;25(12):3561-3571.

65. Nagaya T, Nakamura Y, Okuyama S, et al. Near-Infrared Photoimmunotherapy Targeting Prostate Cancer with Prostate-Specific Membrane Antigen (PSMA) Antibody. *Mol Cancer Res*. 2017;15(9):1153-1162.

66. Maawy AA, Hiroshima Y, Zhang Y, et al. Near infra-red photoimmunotherapy with anti-CEA-IR700 results in extensive tumor lysis and a significant decrease in tumor burden in orthotopic mouse models of pancreatic cancer. *PLoS One*. 2015;10(3):e0121989.

67. Hanaoka H, Nagaya T, Sato K, et al. Glypican-3 targeted human heavy chain antibody as a drug carrier for hepatocellular carcinoma therapy. *Mol Pharm*. 2015;12(6):2151-2157.

68. Sato K, Choyke PL, Kobayashi H. Photoimmunotherapy of gastric cancer peritoneal carcinomatosis in a mouse model. *PLoS One*. 2014;9(11):e113276.

69. Wei D, Tao Z, Shi Q, et al. Selective Photokilling of Colorectal Tumors by Near-Infrared Photoimmunotherapy with a GPA33-Targeted Single-Chain Antibody Variable Fragment Conjugate. *Mol Pharm*. 2020;17(7):2508-2517.

70. Sato K, Nagaya T, Choyke PL, Kobayashi H. Near infrared photoimmunotherapy in the treatment of pleural disseminated NSCLC: preclinical experience. *Theranostics*. 2015;5(7):698-709.

71. Sato K, Nagaya T, Mitsunaga M, Choyke PL, Kobayashi H. Near infrared photoimmunotherapy for lung metastases. *Cancer Lett*. 2015;365(1):112-121.

72. Sato K, Nagaya T, Nakamura Y, Harada T, Choyke PL, Kobayashi H. Near infrared photoimmunotherapy prevents lung cancer metastases in a murine model. *Oncotarget*. 2015;6(23):19747-19758.

73. Nagaya T, Nakamura Y, Sato K, et al. Near infrared photoimmunotherapy with avelumab, an anti-programmed death-ligand 1 (PD-L1) antibody. *Oncotarget*. 2017;8(5):8807-8817.

74. Nakamura Y, Ohler ZW, Householder D, et al. Near Infrared Photoimmunotherapy in a Transgenic Mouse Model of Spontaneous Epidermal Growth Factor Receptor (EGFR)-expressing Lung Cancer. *Mol Cancer Ther*. 2017;16(2):408-414.

75. Nagaya T, Nakamura Y, Okuyama S, et al. Syngeneic Mouse Models of Oral Cancer Are Effectively Targeted by Anti-CD44-Based NIR-PIT. *Mol Cancer Res*. 2017;15(12):1667-1677.

76. Sato K, Hanaoka H, Watanabe R, Nakajima T, Choyke PL, Kobayashi H. Near infrared photoimmunotherapy in the treatment of disseminated peritoneal ovarian cancer. *Mol Cancer Ther*. 2015;14(1):141-150.

77. Nagaya T, Sato K, Harada T, Nakamura Y, Choyke PL, Kobayashi H. Near Infrared Photoimmunotherapy Targeting EGFR Positive Triple Negative Breast Cancer: Optimizing the Conjugate-Light Regimen. *PLoS One*. 2015;10(8):e0136829.

78. Jin J, Krishnamachary B, Mironchik Y, Kobayashi H, Bhujwalla ZM. Phototheranostics of CD44-positive cell populations in triple negative breast cancer. *Sci Rep*. 2016;6:27871.

79. Yamaguchi H, Pantarat N, Suzuki T, Evdokiou A. Near-Infrared Photoimmunotherapy Using a Small Protein Mimetic for HER2-Overexpressing Breast Cancer. *Int J Mol Sci*. 2019;20(23):5835.

80. Jing H, Weidensteiner C, Reichardt W, et al. Imaging and Selective Elimination of Glioblastoma Stem Cells with Theranostic Near-Infrared-Labeled CD133-Specific Antibodies. *Theranostics*. 2016;6(6):862-874.

81. Burley TA, Mączyńska J, Shah A, et al. Near-infrared photoimmunotherapy targeting EGFR-Shedding new light on glioblastoma treatment. *Int J Cancer*. 2018;142(11):2363-2374.

82. Sievers E.L., Senter P.D. Antibody-Drug Conjugates in Cancer Therapy. *Annu. Rev. Med.* 2013;64:15–29.

83. Chau C.H., Steeg P.S., Figg W.D. Antibody–drug conjugates for cancer. *Lancet.* 2019;394:793–804.

84. Beck A, Goetsch L, Dumontet C, Corvaïa N. Strategies and challenges for the next generation of antibody–drug conjugates. Nat Rev Drug Discov. 2017;16:315–37.

85. McCombs JR, Owen SC. Antibody drug conjugates: design and selection of linker, payload and conjugation chemistry. AAPS J. 2015;17:339–51.

86. Doronina SO, Toki BE, Torgov MY, et al. Development of potent monoclonal antibody auristatin conjugates for cancer therapy. Nat Biotechnol. 2003;21:778–84.

87. Welborn M, Duvic M. Antibody-Based Therapies for Cutaneous T-Cell Lymphoma. Am. J. Clin. Dermatol. Springer International Publishing; 2019. p. 115–122.

88. Alaibac M. Monoclonal antibodies against cutaneous T-cell lymphomas. Expert Opin. Biol. Ther. 2017;17:1503–1510.

89. Yoshie O, Matsushima K. CCR4 and its ligands: from bench to bedside. Int. Immunol. 2015;27:11–20.

90. Oka T, Miyagaki T. Novel and Future Therapeutic Drugs for Advanced Mycosis Fungoides and Sezary Syndrome. Front. Med. 2019;6:116.

91. Moore DC, Elmes JB, Shibu PA, Larck C, Park SI. Mogamulizumab: An Anti-CC Chemokine Receptor 4 Antibody for T-Cell Lymphomas. Ann Pharmacother. 2020 Apr;54(4):371-379.

92. Gébleux R, Stringhini M, Casanova R, Soltermann A, Neri D. Non-internalizing antibody-drug conjugates display potent anti-cancer activity upon proteolytic release of monomethyl auristatin E in the subendothelial extracellular matrix. Int J Cancer. 2017 Apr 1;140(7):1670-1679.

93. Prince HM, Kim YH, Horwitz SM, Dummer R, Scarisbrick J, Quaglino P, et al. Brentuximab vedotin or physician's choice in CD30-positive cutaneous T-cell lymphoma (ALCANZA): an international, open-label, randomised, phase 3, multicentre trial. The Lancet. 2017;390(10094):555-66.